Cardiomyocyte calcineurin is required for the onset and progression of cardiac hypertrophy and fibrosis in adult mice

Sara Martínez-Martínez PhD[a,b†], Noelia Lozano-Vidal PhD[a†], María Dolores López-Maderuelo PhD[a,b], Luis Jesús Jiménez-Borreguero MD[b,c], Ángel Luis Armesilla PhD[b,d] and Juan Miguel Redondo PhD[a,b*].

[a]Gene regulation in cardiovascular remodeling and inflammation group, Centro Nacional de Investigaciones Cardiovasculares Carlos III (CNIC), Madrid, Spain
[b]Centro de Investigaciones Biomédicas en RED en Enfermedades Cardiovasculares (CIBERCV), Spain.
[c]Hospital de La Princesa, Madrid, Spain.
[d]Research Institute in Healthcare Science, School of Pharmacy, Faculty of Science and Engineering, University of Wolverhampton, Wolverhampton, United Kingdom

Corresponding author.
[†] S. Martínez-Martínez and N. Lozano-Vidal contributed equally to this work.

Address for correspondence: Dr Juan Miguel Redondo, Gene regulation in cardiovascular remodeling and inflammation group, Centro Nacional de Investigaciones Cardiovasculares Carlos III (CNIC), Melchor Fernández Almagro 3, 28029 Madrid, Spain.
Tel: (+34) 91 453 1200 ext
Fax: (+34) 91 453 1265

Running title: Cardiomyocyte calcineurin in cardiac hypertrophy.

Keywords: heart, cyclosporin A, pro-fibrotic genes, angiotensin II**.**

ABBREVIATIONS LIST

IGF1= insulin-like growth factor 1

PI3K=Phosphatidylinositol-4,5-bisphosphate 3-kinase

AKT= Protein Kinase B

ERK1/2= extracellular signal–regulated kinases 1/2

AMPK= AMP-activated protein kinase

mTOR= mammalian Target of Rapamycin

MAPK= mitogen-activated protein kinase

NFAT= nuclear factor of activated T cells

GRK= GPCR receptor kinases

PDE5= phosphodiesterase 5

PKCα= Protein kinase C alpha

CaMKII= Ca2+/calmodulin-dependent kinase II

***Myh6*=** myosin, heavy polypeptide 6, cardiac muscle, alpha

Rcan1.4= regulator of calcineurin 1.4

***Ptgs-2*=** prostaglandin-endoperoxide synthase 2

Cox-2= cyclooxygenase 2

***Col3a1*=** collagen, type III, alpha 1

***Col1a1*=** collagen, type I, alpha 1

p38 MAPK= mitogen-activated protein kinase p38

Jnk= c-jun N-terminal kinase

Tgfβ= transforming growth factor beta

ABSTRACT

Previous studies have demonstrated that activation of calcineurin induces pathological cardiac hypertrophy. In these studies, loss-of-function was mostly achieved by systemic administration of the calcineurin inhibitor cyclosporin A. The lack of conditional knockout models for calcineurin function has impeded progress toward defining the role of this protein during the onset and the development of cardiac hypertrophy in adults. Here, we exploited a mouse model of cardiac hypertrophy based on the infusion of a hypertensive dose of angiotensin II (AngII) to model the role of calcineurin in cardiac hypertrophy in adulthood. AngII-induced cardiac hypertrophy in adult mice was reduced by treatment with cyclosporin A, without affecting the associated increase in blood pressure, and also by induction of calcineurin deletion in adult mouse cardiomyocytes, indicating that cardiomyocyte calcineurin is required for AngII-induced cardiac hypertrophy. Surprisingly, cardiac-specific delection of calcineurin, but not treatment of mice with cyclosporin A, significantly reduced AngII-induced cardiac fibrosis and apoptosis. Analysis of pro-fibrotic genes revealed that AngII-induced expression of *Tgfβ*-family members and *Lox* was not inhibited by cyclosporin A but was markedly reduced by cardiac-specific calcineurin deletion. These results show that AngII induces a direct, calcineurin-dependent pro-hypertrophic effect in cardiomyocytes, as well as a systemic hypertensive effect that is independent of calcineurin activity.

1. INTRODUCTION

Cardiac hypertrophy (CH) is the main mechanism by which the heart reduces stress on the ventricular walls [1-3]. In the initial response to cardiac overload, heart function is maintained through increased protein synthesis and cardiomyocyte enlargement, accompanied by sarcomere reorganization. This cardiac response can be induced in physiological or pathological situations. During pregnancy or intensive exercise training, CH is an advantageous adaptation; however, in response to hypertension, aortic stenosis, or myocardial infarction, the initial compensatory response to cardiac stress becomes maladaptive and constitutes a major risk for the development of heart failure [4].

The precise mechanisms underlying physiological and pathological CH are not fully understood; however, pathological cardiac remodeling is characterized by the development of fibrosis that contributes to loss of heart function. Several studies indicate that physiological and pathological cardiac remodeling involve different biochemical stimuli and intracellular signaling pathways, which could explain their differing outcomes [1-3]. Physiological cardiac hypertrophy is triggered by a limited number of growth factors (thyroid hormone, insulin, insulin-like growth factor 1 and vascular endothelial growth factor) and mechanical stimuli that activate the IGF1/PI3K/AKT, ERK1/2, AMPK, and mTOR-dependent signaling pathways. In contrast, pathological hypertrophy is activated by a plethora of neuro-hormonal factors and biomechanical stimuli and intracellular pathways, including MAPK kinases, GRK, PDE5, PKCα, CAMKII, and Ca^{2+}-dependent effectors. Prominent inducers of pathological CH include the calcium-calmodulin-dependent phosphatase calcineurin (Cn) and its substrate NFAT [5]. Although numerous gain-of-function studies have demonstrated that Cn and NFAT both induce a pathological phenotype involving cardiac growth [5, 6], most loss-of-function experiments have been performed with the pharmacological Cn inhibitors cyclosporin A (CsA) and FK506 (tacrolimus) or mice constitutively lacking Cn or NFAT [5]. To date, 2 studies have described the generation of mice with cardiac-specific loss of Cn in the heart, by deletion of the *Cnb1* gene [7, 8]. However, the use of a non-inducible cardiomyocyte driver in these mice causes cardiac Cn deletion in the perinatal period, when cardiomyocytes are proliferating [9], resulting in depressed cardiac function and 50% lethality at 4-6 months [7, 8]. To our knowledge, no mouse model to date has modeled the role of cardiac Cn during CH in adulthood, when the disease develops.

Hypertension is a major inducer of pathological cardiac remodeling characterized by left ventricular hypertrophy and cardiac fibrosis [4, 10]. High blood pressure, such as that induced by angiotensin II (AngII), is a well-known mediator of CH [11]. Recent evidence suggests that AngII also exerts a pressor-independent and direct action on cardiac remodelling [12-14]. Previous studies in animal models of hypertension demonstrated the participation of Cn in CH [15-17]; however, the precise role of Cn in CH onset and progression has not been defined. For the present study, we generated a mouse model of inducible and cardiac-specific *Cn* deletion.

Through a combination of genetic experimental and pharmacological approaches, we show that Cn plays an essential role in the development of AngII-mediated CH, whereas cardiac fibrosis is mediated by CsA-insensitive mechanisms involving members of the Tgfβ and Lox families.

2. RESULTS

2.1. A Cn-inhibitory CsA concentration reduces AngII-induced cardiac hypertrophy in mice without affecting hypertension.

CsA at higher doses than those used therapeutically to achieve Cn inhibition and immunosuppression [18, 19] reduces CH induced by non-pressor doses of AngII in rats [20]. We therefore tested whether lower (clinical) doses of CsA would prevent CH induced by pro-hypertensive AngII concentrations. We treated wild-type mice for 21 days with AngII (60 μg/kg/h) and a pharmacological CsA dose (0.208 mg/kg/h). This CsA dose is 10-fold below that used in rats [20]. AngII induced an increase in systolic blood pressure (**Table 1**) that was unaffected by co-treatment with CsA (**Table 1**). Postmortem analysis revealed a significant AngII-induced increase in ventricular mass that was inhibited by CsA (**Fig. 1A**).

To determine whether the AngII-induced increase in cardiac mass was due to increased cardiomyocyte size, we measured cardiomyocyte cell area in cardiac cross-sections. Cardiomyocyte area was significantly enlarged in AngII-infused mice, and this increase was again attenuated by CsA (**Fig. 1B**). Consistent with these morphological data, echocardiography in live AngII-infused mice revealed notable increases in left ventricular posterior wall (LVPW) and interventricular septum (IVS) thickness (**Table 1**). CsA did not modify ventricular wall thickness in sham-implanted animals, but attenuated the increase in wall thickness induced by AngII infusion (**Table 1**). Analysis of ejection fraction (EF) revealed that AngII and CsA treatment had no significant impact on systolic cardiac function (**Table 1**).

These results suggest that Cn activation plays an important role in AngII-induced CH and indicate that pharmacological Cn inhibition with CsA significantly reduces cardiac enlargement without reverting AngII-induced hypertension.

2.2. AngII triggers early activation of Cn-dependent gene expression and the cardiac hypertrophy program

We next investigated whether AngII activates Cn-dependent gene expression in the heart. Cardiac mRNA expression of the Cn target genes *Rcan1.4* and *Ptgs-2* [21, 22] was elevated in wild-type mice after AngII treatment for 15 h, decreasing to basal levels after 3 days (**Fig. 2A**). This transcriptional effect was reflected in the induction of cardiac Rcan1.4 and Cox-2 protein expression as soon as 1 day after treatment (**Fig. 2B and 2C**). Rcan1.4 expression returned to baseline levels after 2 days of AngII infusion, whereas maximum Cox2 expression was maintained at this time (**Fig. 2C**). Treatment with either a low CsA dose (0.208 mg/kg/h) or a high CsA dose (0.832 mg/kg/h) markedly reduced AngII-induced cardiac Rcan1.4 and Cox2 expression (**Fig. 2B and 2C**), suggesting that Cn activation was required for their upregulation.

Given that AngII induced a very early activation of cardiac Cn-dependent gene expression, we analyzed whether AngII treatment also results in an early development of the hypertrophic phenotype. CH development

was monitored in wild-type mice treated with AngII for 1 or 3 days. Notably, as early as 3 days after the initiation of AngII infusion, mice showed significant increases in ventricular mass (**Fig. 2D**), cardiomyocyte area (**Fig. 2E**), and IVS thickness (**Fig. 2F**). This early AngII-induced CH was attenuated by treatment with CsA (**Fig. 2D-F**).

These results show that AngII induces an early expression of Cn-dependent genes in the heart that is concomitant with the early appearance of a CH phenotype. The blockade of these effects with Cn inhibitors suggests that activation of Cn signaling mediates AngII-induced CH.

2.3. AngII-induced CH requires cardiomyocyte Cn.

Although our experiments were performed with low CsA concentration, this immunosuppressant can have effects unrelated to Cn and might interfere with targets others than Cn [23]. Knockout models in principle represent a more precise alternative to the use of pharmacological Cn inhibitors. However, none of the reported mouse models allows study of the role of Cn in the development of CH, a condition of adulthood: mice systemically lacking *Cnb1* die during embryogenesis [24], and Cn deletion using the alpha-myosin heavy chain (*Myh6*) promoter results in death in early-mid adulthood [7, 8]. To address this issue, we generated a mouse model allowing induced cardiomyocyte-specific deletion of floxed *Cnb1*. In these mice *Cnb1* deletion is induced in cardiomyocytes expressing Cre recombinase under the control of the *Myh6* promoter in a tamoxifen-inducible manner. $Cnb1^{\Delta/flox}$ mice [25] were crossed with $Myh6^{CreERT2}$ mice [26] to obtain $Cnb1^{\Delta/flox}$; $Myh6^{CreERT2}$ mice or $Cnb1^{flox/flox}$; $Myh6^{CreERT2}$ mice, hereafter called Cnb1-$flox^{Myh6}$ mice (details in Methods). Treatment of Cnb1-$flox^{Myh6}$ mice with 4-hydroxy tamoxifen (Tx) strongly reduced cardiac Cnb1 mRNA and protein expression (**Fig. S1A and Fig. 3A**). Western blot analysis revealed unaltered CnB protein expression in thymus, aorta, liver, and kidney of Tx-treated Cnb1-$flox^{Myh6}$ mice (**Fig. 3B**), confirming specific deletion in cardiac tissue. The destabilization of the catalytic subunit CnA in the absence of the regulatory subunit CnB has been previously demonstrated in *in vivo* models [7, 27]**.** Similarly, we confirmed that the deletion of cardiac *Cnb1* expression resulted in similar reduction of the protein levels of both CnB and CnA (**Fig. 3A** and **Fig. S1B**).

Having confirmed the specificity and efficacy of *Cn* deletion in Tx-treated Cnb1-$flox^{Myh6}$ mice, we infused them with AngII for 1 day and determined the cardiac mRNA expression of the Cn target genes *Rcan1.4* and *Ptgs2*, as an index of Cn pathway activity. *Rcan1.4* and *Ptgs2* mRNA levels were markedly lower in Tx-treated mice than in untreated controls (**Fig. 3C**), and similar results were obtained for Rcan1.4 protein (**Fig. 3D**), suggesting that inducible, cardiac-specific Cn ablation inhibits the expression of Cn-dependent genes in the hearts of AngII-treated mice.

We next analyzed the effect of cardiac *Cnb1* deletion in adult mice on AngII-induced CH. Mice treated with Tx or vehicle were infused with AngII for 21 days. The induced loss of cardiac Cn diminished AngII-induced

increases in ventricular mass and cardiomyocyte cross-sectional area (**Fig. 4A and 4B**), and echocardiography confirmed attenuation of the AngII-induced increase in left ventricular wall thickness (**Table 2**). Induced cardiac *Cnb1* deletion was equally effective as CsA-mediated inhibition of Cn phosphatase activity at preventing AngII-induced CH.

These results implicate cardiomyocyte Cn in CH and validate Cnb1-flox^{Myh6} mice as a model for investigating the mechanisms underlying the onset and progression of hypertrophy in the adult heart.

2.4. *Cardiac Cn mediates AngII-induced fibrosis and pro-fibrotic gene expression*.

Cardiac fibrosis—the abnormal accumulation of extracellular matrix proteins (ECM) such as collagens and fibronectins in the myocardium—is a common feature of pathological CH [2]. In wild-type mice, AngII treatment for 21 days induced significant myocardial fibrosis that was not prevented by CsA (**Fig. 5A**). Histological analysis at earlier time points revealed marked cardiac fibrosis on day 3 of AngII stimulation; CsA not only did not prevent this but seemed to exacerbate it (**Fig. 5B**). The histological data correlated with the mRNA expression of *Col3a1*, which encodes one of the two fibrillar collagen types that form the myocardial extracellular matrix (**Fig. 5C**). These results suggest that AngII-induced cardiac fibrosis is Cn-independent; however, AngII-mediated cardiac fibrosis was strongly reduced by Cn deletion in the cardiomyocytes of Cnb1-flox^{Myh6} mice (**Fig. 5D**). As in wild type mice, CsA did not prevent AngII-induced heart fibrosis in Cnb1-flox^{Myh6} mice, demonstrating that the divergence between the results obtained with pharmacological and genetic Cn inhibition was not due to the use of different mouse strains (**Fig. 5D**). As observed in mice treated with AngII for 21 days, the cardiac *Cnb1* deletion attenuated CH and fibrosis as early as 3 days after AngII infusion (**Fig. 6**).

Cardiomyocyte death has been described as a possible mechanism responsible for induction of the fibrotic response [28], and the presence of apoptotic cells in cardiac tissue has been widely reported in AngII-treated rodents [11, 29, 30]. TUNEL assays to evalute the extent of apoptosis in AngII-treated mice in the pharmacological and genetic models revealed a significant increase in the number of apoptotic cells after 3 days of AngII-treatment (**Fig. 7A and 7B**). Similar to the fibrotic response, AngII-induced heart apoptosis was unaffected by CsA and was prevented by Cn deletion in cardiomyocytes (**Fig. 7A and 7B**). Apoptosis and fibrosis thus show the same divergence in the response to pharmacological and genetic Cn inhibition.

The elevated and abnormal deposition of collagens during cardiac fibrosis is regulated at the levels of synthesis, maturation, and degradation [31]. Cytokines and growth factors implicated in fibrosis induction include interleukin-6 (Il-6) and members of the Tgfβ family [32]. We therefore examined whether the expression of pro-fibrotic genes was differently affected by pharmacological and genetic Cn inhibition during AngII-induced cardiac fibrosis. Gene expression of *Il-6*, *Tgfβ1*, *Tgfβ2*, and the Tgfβ-induced gene *Tgfβi* was significantly upregulated in the hearts of wild type mice after 1 day of AngII infusion, whereas *Tgfβ3* mRNA was

significantly increased after AngII infusion for 3 days (**Fig. 8A**). Analysis of gene expression in the hearts of Tx-treated Cnb1-flox^{Myh6} mice and CsA-treated wild-type mice revealed suppression of AngII-induced *Il-6* expression in both cases, whereas AngII-induced *Tgfβ3* upregulation was unaffected (**Fig. 8B**). In contrast, AngII-induced *Tgfβ1*, *Tgfβ2*, and *Tgfβi* expression was not inhibited by CsA in wild-type mice but was reduced by cardiac-specific *Cnb1* deletion (**Fig. 8B**). *Tgfβ* family members can trigger the activation and maturation of collagen expression [32], suggesting that the differential *Tgfβ* expression pattern might underlie the divergent fibrotic phenotypes observed. However, AngII-induced mRNA expression of *Col1a1* and *Col3a1* was not reduced in response to cardiac *Cnb1* deletion, and CsA further potentiated their expression (**Fig. 8C**).
Processing of collagens into mature fibrils requires covalent cross-linking mediated by members of the lysyl oxidase family [33], the most prominent member is Lox. AngII-induced upregulation of *Lox* mRNA expression was not affected by CsA treatment in wild type mice, but was significantly decreased by deletion of cardiomyocyte Cn (**Fig. 8D**). This pattern was reflected at the protein level, with AngII-induced Lox protein expression not reduced by CsA, and even increased, whereas cardiac *Cnb1* deletion blunted this upregulation (**Fig. 8E**). As reported for transaortic constriction-induced CH [34], AngII also upregulated the other *Lox* family members (*Loxl1*, *Loxl2*, *Loxl3*, and *Loxl4*) in the heart (**Fig. 9**). Cardiac *Cnb1* deletion blocked AngII-induced upregulation of *Loxl4*, but not *Loxl1, Loxl2*, or *Loxl3* (**Fig. 9**).
These results indicate that cardiomyocyte Cn regulates AngII-induced cardiac fibrosis and expression of essential pro-fibrotic genes in murine heart.

3. DISCUSSION

In this study, we provide evidence demonstrating that AngII at hypertensive doses activates Cn signaling in the mouse heart concurrently with the development of cardiac hypertrophy. Remarkably, inhibition of Cn with low CsA doses impaired AngII-induced CH but did not reverse the associated blood pressure increase, suggesting that AngII exerts a direct Cn-dependent pro-hypertrophic effect on cardiac cells and an indirect Cn-independent hypertensive effect. These results are consistent with CsA-mediated reduction of AngII-linked CH in other mouse models, including renal damage-induced CH [16] and aldosterone-induced CH [17]. Our findings indicate that in a pathological setting AngII directly activates specific pro-hypertrophic pathways in cardiac cells that differ from those triggered by hypertension-derived hemodynamic stimuli. Supporting this idea, subpressor AngII doses induce CH in rats [20]. Furthermore, AngII-dependent activation of p38 MAPK signaling has been linked to a direct action on mouse cardiac cells, whereas activation of Erk and Jnk is linked to AngII-induced mechanical stress on the heart [35]. These results suggest that treatment of pathological cardiac hypertrophy in patients presenting high blood pressure would require blockade of specific intracellular pathways activated by hypertension-independent mechanisms.

Pharmacological inhibition of Cn with CsA is a useful tool for investigating the involvement of Cn in CH progression. However, systemic drug delivery does not target the specific contribution of cardiac Cn. Here, we explored the precise implication of cardiac Cn in the onset and progression of CH in adulthood, using a newly generated mouse model of inducible cardiomyocyte-specific *Cnb1* deletion, based on floxed *Cnb1* and Cre recombinase expression under the control of the inducible cardiac promoter *Myh6*. In this mouse model, deletion of CnA and CnB occurs in a similar manner, which implies that Cn-mediated phosphatase activity in the heart is inhibited upon conditional deletion of *Cnb1*, as this also led to the loss of the Cn catalytic subunit (CnA). These results therefore suggest that genetic and pharmacological approaches both result in the inhibition of Cn activity.

We have found that conditional deletion of cardiomyocyte *Cnb1* prevents AngII-induced CH. These results are consistent with previous reports showing inhibition of AngII-mediated heart weight gain in mouse models with constitutive deficiency of the catalytic subunit CnAβ or the Cn substrates NFATc3 or NFATc2 [36-38]. However, it is important to note that these studies examined induction of CH by pressure-overload or Cn-overexpression, which are not mediated by systemic hypertension, and AngII was used only to confirm that deletion of these Cn/NFAT signaling pathway components were involved in AngII-mediated heart weight increase. Here, we have characterized the cardiac hypertrophy induced by a well-characterized pro-hypertensive dose of AngII [39-42] and analyzed the role of cardiomyocyte Cn in cardiomyocyte size, ventricular wall thickness, fibrosis, expression of pro-fibrotic genes, and apoptosis. Our data indicate that cardiomyocyte Cn in

adulthood regulates cardiac remodeling and function during the onset and development of AngII-mediated cardiac hypertrophy.

Remarkably, cardiac-specific Cn deletion in healthy adult mice did not impair cardiac function (Tx-treated sham-implanted Cnb1-flox^{Myh6} mice, Table 2). A cardiac-specific Cn knockout mouse was recently generated [7, 8], but in this model, cardiac Cn deletion is not inducible and begins at the perinatal stage, resulting in impaired contractility and cardiac growth, and death between 4 and 6 months after birth [7, 8]. The differences between these results and ours suggest that Cn plays different roles in cardiac homeostasis during postnatal development and adulthood and are consistent with data showing that Cn signaling differs between neonatal and adult cardiomyocytes [43].

Although most animal models of CH are based on chronic stimulation, we show here that mice display Cn-dependent CH markers as soon as 3 days after AngII infusion (**Fig. 2 and Fig. 6**). Our results show that AngII-induced activation of cardiac Cn mediates CH progression from the onset of the disease. We also found that Cn inhibition by CsA infusion or cardiac-specific *Cnb1* deletion prevents AngII-induced cardiomyocyte hypertrophy. However, these 2 approaches to Cn inhibition have divergent effects on AngII-induced cardiac fibrosis, which was unaffected by CsA but impaired by cardiac-specific *Cnb1* deletion. In fact, our results in fibrosis using genetic approach are consistent with those obtained by overexpressing specifically in heart the Cn inhibitor, RCAN1 [44].

The effect of CsA treatment on different CH models has broadly been studied, obtaining controversial results about its CH inhibitory capacity [45]. Most studies that describe a CsA inhibitory effect on CH does not focus on its effect on fibrotic process induced in CH, and few studies that analyze it show opposing results. CsA-mediated fibrosis attenuation [15] and exacerbation [46] have been described in AngII-non linked CH, while there is only one study in which it is described that CsA inhibits cardiac fibrosis mediated by an AngII-linked model, uninephrectomized and aldosterone-treated rats [17]. However, the result of systemic pharmacological inhibition of Cn on AngII-induced cardiac fibrosis has not been analyzed until the present work. The different doses of CsA and/ or different hypertrophic stimuli used in these studies could explain the discrepancies found. Several studies have described myocardial fibrosis as a potential CsA side effect [46, 47], providing a possible explanation for the fibrotic phenotype in CsA-treated animals. However, this is unlikely to be the case in our experiments because CsA did not increase myocardial fibrosis in sham-implanted wild-type animals. In previous studies showing CsA-promoted fibrosis [46-48], the experiments used much higher CsA concentrations than those used here, suggesting that the pro-fibrotic effects might represent off-target effects on molecules other than Cn [23, 49]. Cardiac fibrosis induction can be in part a response to cell death [28], and high doses of CsA induces apoptosis [50]. In our genetic and pharmacological models, we found that the apoptotic and fibrotic responses follow a similar pattern in both experimental settings, and that CsA *per se* does

not induce apoptosis. CsA has also been found to increase Tgf-β1 levels in biopsies from immunosuppressed patients, animal models, and cells exposed to the drug *in vitro* [51-53]. A mechanism proposed for this effect is CsA-enhanced Tgf-β1 synthesis. However, in mice treated with CsA alone we detected no increase in cardiac *Tgfβ1* mRNA (data not shown). Although we observed no CsA-mediated effect that explains the fibrosis results in CsA/AngII-treated mice, we cannot exclude the possibility that CsA posttranscriptionally or posttranslationally modifies a factor or factors involved in fibrosis [54, 55], producing an effect that is insufficient to induce fibrosis on its own but sufficient to maintain the induction of *Tgfβ*/fibrosis mediated by AngII.

An alternative hypothesis consistent with our results is that, in addition to its well-known phosphatase action, cardiac Cn is essential for the assembly of molecular signaling complexes in specific cardiomyocyte subdomains that could be implicated in AngII-induced fibrosis. Supporting this idea, anchoring of Cn to the sarcomere Z-disc is critical for the integration of cardiomyocyte stress signals [43]. Other possible explanation for divergent effects on AngII-induced cardiac fibrosis in two approaches to Cn inhibition may lie in the intricate intercellular crosstalk between fibroblasts and cardiomyocytes that has been described during AngII-cardiac remodelling [56]. In contrast to cardiomyocyte-specific *Cnb1* deletion, systemic inhibition of Cn mediated by CsA could have adverse profibrotic effect in other cell types of the heart or reveal differences in the Cn susceptibility to its activity inhibition by CsA depending on the cellular context in the similar way that differences in susceptibility of each tissue has been described [57]. Advances in the generation of Cre-recombinase gene-targeted mice are enabling specific genetic manipulation of fibroblasts or differentiated myofibroblasts [58]. Future experiments taking avantage of these advances will allow us to explore the contribution of this cardiac cellular comparment to the observed fibrotic effects and to analyze possible differences in Cn susceptibilitly to drug-mediated inhibition depending on each cellular compartment.

In recent years, new factors have been identified and characterized that trigger and maintain the myocardial fibrotic response in different cardiac diseases [59]. An important role in pathological cardiac fibrosis was recently described for the lysyl oxidase (Lox) family of enzymes, which catalyze collagen assembly [34, 60-63]. Here we show that suppression of cardiac Cn impairs the transcriptional expression of *Lox*, which is involved in the progression of a pathological fibrotic response in the heart. However, CsA-mediated Cn inactivation does not affect the expression of *Lox*-family genes or the appearance of a fibrotic phenotype in the injured heart. The inhibition of AngII-induced cardiac fibrosis after cardiac-specific *Cnb1* deletion likely involves the regulation of numerous genes; however, the marked inhibition of *Tgfβ* family members and *Lox* gene expression could probably account by itself for the decrease in the fibrotic phenotype. Tgfβ has been identified as an important upregulator of Lox enzymes in several cell types and tissues [62, 64-66]. Therefore the effect of Cn deletion on the cardiac expression of *Tgfβ* members could also underlie the Lox-mediated reduction of collagen fiber

maturation. Thus, the observed effects on fibrosis induction could reflect the direct fibroblast response to changes in *Tgfβ* or Lox expression. However, the effect of Cn deletion on the AngII-mediated apoptotic response in our experiments does not exclude the possibility that the inhibition of fibrosis in the absence of cardiomyocyte Cn is due in part to interference in AngII-induced cell death. This study reports a novel role of cardiomyocyte Cn, showing that Cn regulates pro-fibrotic gene expression and the progression of pathological cardiac fibrosis. Cardiac-specific Cn suppression is a potentially attractive therapeutic strategy. Future experiments will be required to clarify why cardiac fibrosis is inhibited by Cn genetic deletion but not by treatment with CsA, and future research is thus warranted into adeno-associated virus type 9-based clinical interventions for siRNA-mediated suppression of cardiomyocyte Cn expression. Our results highlight the importance of targeting Cn expression in the design of novel clinical interventions to prevent fibrosis in the injured heart, and also suggest that therapeutic strategies by targeting Lox should be explored.

4. MATERIAL AND METHODS

4.1. Animals

All animal studies were conducted in accordance with EU Directive 2010/63/EU and Recommendation 2007/526/EC regarding the protection of animals used for experimental and other scientific purposes, enforced in Spanish law under Real Decreto 1201/2005. C57BL/6J mice were obtained from Charles River laboratories. To delete Cn specifically in cardiomyocytes, we crossed $Cnb1^{\Delta/flox}$ mice [25], in which one *Cnb1* allele is deleted and the remaining allele is floxed, with $Myh6^{CreERT2}$ transgenic mice [26] to obtain $Cnb1^{\Delta/flox}$; $Myh6^{CreERT2}$ or $Cnb1^{flox/flox}$; $Myh6^{CreERT2}$ mice containing a floxed-version of the *Cnb1* gene (Table in **Fig. S1)**. Gross phenotype was assessed in animals of both genotypes maintained to the age of 6 months. In the absence of Cre-activation–induced *Cnb1* deletion, mice with a single floxed *Cnb1* allele ($Cnb1^{\Delta/flox}$) and mice with 2 floxed *Cnb1* alleles ($Cnb1^{flox/flox}$) showed no significant differences in survival (**Fig. S1C**). As expected *Cnb1* mRNA levels in $Cnb1^{\Delta/flox}$ mice were 50% of those of $Cnb1^{flox/flox}$ mice (**Fig. S1A**), however, similar CnB protein levels were detected in the different tissues analyzed, irrespective of the presence of one or two alleles *Cnb1* gene, supporting haplo-sufficiency for the *Cnb1* gene (**Fig. S1D**). After the Cre recombinase activation by 4-hydroxy tamoxifen (Tx, Sigma-Aldrich, St.Louis, MO, USA, H6278) administration, both genotypes ($Cnb1^{\Delta/flox}$; $Myh6^{CreERT2}$ and $Cnb1^{flox/flox}$; $Myh6^{CreERT2}$ mice) showed similar reductions in the levels of cardiac *Cnb1* mRNA (**Fig. S1A**) and cardiac CnB and CnA protein (**Fig. S1B**). In $Myh6^{CreERT2}$ mice, Cre recombinase activation in heart *per se* did not affect the expression of CnB and CnA proteins (**Fig. S1E**). Under baseline conditions, both genotypes showed no gross differences in phenotype or CnB and CnA protein expression, and both genotypes also displayed similar deletion levels of cardiac CnB after Cre activation; we therefore used mice of both genotypes in our experiments, hereafter referred to as Cnb1-$flox^{Myh6}$ mice.

To achieve specific *Cnb1* gene deletion in cardiomyocytes, Cnb1-$flox^{Myh6}$ mice were injected intraperitoneally (ip.) with 40 mg/kg/day of Tx in corn oil [67] for 5 consecutive days between the ages of 8 and 12 weeks. To avoid interference from Cre activation or Tx treatment, experiments were conducted at least 2 weeks after the last Tx injection.

4.2. AngII treatment in vivo

Mice were anesthetized with 1.5% sevoflurane and fitted subcutaneously beneath the scapula with osmotic minipumps (model 2001 and 2004 Alzet; Durect Corporation, Cupernico, CA, USA) containing AngII (Sigma-Aldrich, St.Louis, MO, USA, A9525, 60 µg/kg/h) or CsA (Novartis, Switzerland, 0.208 mg/kg/h). CsA-containing minipumps were implanted 2 days before AngII minipumps to ensure pharmacological Cn inhibition before AngII administration. Control mice underwent the same surgical procedure but without minipump implantation (sham-implanted mice) [68].

Mice were weighed and sacrificed after 1, 3, or 21 days of AngII treatment. Hearts were removed and the atria excised. The ventricles were weighed and dissected, with one part being processed for histology and another snap-frozen in liquid nitrogen for protein and RNA analysis. Liver, aorta, thymus and kidneys were also collected in liquid nitrogen. Tibias from left posterior limbs were isolated and measured with a digital caliper.

4.3. Echocardiography

Mice were lightly anesthetized with 1.5% isoflurane. Echocardiography was performed in the parasternal long-axis view using the Vevo 2100 System (VisualSonics Inc., Toronto, Ontario, Canada) with a 30 MHz MS-400 transducer in the 2-dimensional guided M-mode. Measurements were taken of diastolic interventricular and left ventricular posterior wall thicknesses, diastolic left ventricular diameter, and left ventricular ejection fraction.

4.4 Blood pressure

Blood pressure and heart rate measurements were obtained using a noninvasive computerized tail-cuff system (BP-2000, Visitech Systems, NC, USA). Conscious mice from each group were placed on a warming plate and a cuff with a pneumatic pulse sensor was attached to the tail. Mice underwent training for 5 days, and on subsequent days the 10 first readings were discarded, and the mean of the following 10 measurements was calculated.

4.5 Histology

The central portion of the heart was fixed in 10% formalin solution (Sigma-Aldrich, 501128) and then embedded in paraffin. Transverse heart sections (5 μm) were obtained and used for analysis. To measure the cross-sectional area of left ventricular cardiomyocytes, heart sections were stained overnight at 4ºC with 100 μg/ml FITC-conjugated *Triticum vulgaris* lectin (Sigma-Aldrich, L-4895). On each section, images were obtained from 4 fields with a Nikon Eclipse TE 2000-U fluorescence microscope (Nikon, Tokyo, Japan) fitted with a 10x objective. Cardiomyocyte area was calculated from these images using ImageJ [69].

To quantify cardiac fibrosis, serial transverse sections from each ventricle were stained with Picrosirius Red solution (Sigma Aldrich, P-6744-1GA/ 365548-5G) and the fibrotic area in the total section was quantified using ImageJ; fibrosis (red-stained area) was calculated as a percentage of the total section area. In each experiment, values were calculated relative to those from sham-implanted mice.

Apoptosis was detected by terminal dUTP nick-end labeling (TUNEL) assay using the ApopTag® Red In Situ Apoptosis Detection Kit (S7165, Millipore, Temecula, CA, USA) with some modifications. Briefly, apoptosis was detected by staining with PA(phosphatase alkaline)-conjugated anti-digoxigenin antibody. Heart sections were prepared for TUNEL assay according to the manufacturer's instructions. Whole stained heart sections were scanned, and the extent of apoptosis was quantified using NDP.view2 software, Hamamatsu Photonics. The number of apoptotic cells (brown/black nuclei) in myocardium was quantified relative to the total transverse section area (mm^2).

4.6. Western blotting

Total protein from different tissues was extracted by pulverization with the MagnaLyser system (Roche) in lysis buffer (20 mM Tris-HCl pH 7.5, 1% Triton X-100, 50 mM NaF, 5 mM $MgCl_2$, 500 mM NaCl, 10 mM EDTA, and proteases inhibitors: 100 μM benzamidin, 1μg/ml leupeptin, 1 μg/ml pepstatin, 1 μg/ml aprotinin, 1 μM ditiotreitol, 1 mM PMSF, and 3 mM EGTA). Homogenates were incubated on a rocking platform for 30 min at 4ºC and centrifuged for 15 min at 16,000 x *g* at 4ºC, and soluble proteins were collected in the supernatants. Cardiac proteins were extracted in hypotonic buffer as previously described [70]. Briefly, pulverized heart was homogenized with a pestle and glass tube in a morter and pestle in hypotonic lysis buffer (10 mM Hepes pH 7.4, 1.5 mM $MgCl_2$, 10 mM KCl, 0.2% NP-40, 1 mM spermidine, 150 μM spermine, 10 mM MoO_4Na_2, and the protease inhibitors listed above). Homogenates were centrifuged for 15 min at 400 x g at 4ºC, and cytosolic proteins were collected in the supernatants. For both extractions, protein was quantified with the Bradford Protein Assay (Bio-Rad, Hercules, CA, USA).

Proteins from tissue lysates (30-50 μg) were separated by SDS-PAGE and transferred to nitrocellulose membranes. After blocking, the membranes were incubated with specific primary antibodies overnight at 4ºC (anti-Calcineurin B 1:2000, Upstate #cat 05-187; anti-Calcineurin PanA 1:1000, Chemicon #cat ab-1695; anti-α-Tubulin 1:40000, Sigma-Aldrich #cat T-6074; anti-Gadph 1:1000, Abcam, Cambridge, United Kingdom, #cat ab8245; anti-α-Actinin 1:2000, Sigma-Aldrich #cat A-7811; anti-Rcan1 1:1000, Sigma-Aldrich #cat D6694; anti-Cox2 1:1000, Cayman, Ann Arbor, MI, USA, #cat 160126; and anti-Lox 1:2000, Abcam, Cambridge, United Kingdom, #cat ab31238). After washes and incubation with the appropriate specific HRP-conjugated secondary antibodies, immunoreactive bands were visualized using chemiluminescent substrate (ECL western blotting detection reagents, GE Healthcare, Chicago, IL, USA, RPN2106). Specific band intensities were quantified with Quantity One software (Bio-Rad).

4.7. Quantitative RT-PCR

Total RNA was extracted from frozen and pulverized heart tissue using Trisure reagent (Bioline, Bio-38033) and the MagnaLyser system (Roche Life Science, Indianapolis, IN, USA). RNA was quantified and cDNA synthesized using 2 μg of total RNA and M-MLV reverse transcriptase (Promega, Madison, WI, USA, M170B). The resulting cDNA was analyzed by quantitative real-time PCR (qPCR) in an AB7900 sequence detection PCR system (Applied BiosystemFoster City, CA, USA) using SYBR Green PCR (Go Taq qPCR Master Mix, Promega, A600A) or TaqMan Universal PCR (Go Taq Probe PCR Master Mix, Promega, A610A). The following TaqMan probes were used: *Rcan1.4* (Mm01213406_m1, Mm00627762_m1), *Ptgs2* (Mm00478374_m1), *Il6* (Mm00446190_m1), and *Hprt1* (Mm00446968_m1). The specific probes used for SYBR Green detection were as follows: *Cnb1* (5'-TATTCGACACAGACGGCAAC-3' and 5'-CGAAAAGCAAACCTCAACTTC-3'), *Col1a1* (5'-GCTCCTCTTAGGGGCCACT-3' and 5'-

CCACGTCTCACCATTGGGG-3'), *Col3a1* (5'-CTGTAACATGGAAACTGGGGAAA-3' and 5'-CCATAGCTGAACTGAAAACCACC-3'), *Tgfβ1* (5'-CGCCATCTATGAGAAAACC-3' and 5'-GTAACGCCAGGAATTGT-3'), *Tgfβ2* (5'-CCACCTCCCCTCCGAAAA-3', 5'-AGACATCAAAGCGGACGATTCT-3'), *Tgfβ3* (5'-GTCCTCAGTGGAGAAAAATGGAA -3', 5'-TTGGGCACCCGCAAGA-3'), *Tgfβi* (5'-TCCTTGCCTGCGGAAGTG-3', 5'-GGA GAGCATTGAGCAGTTCGA-3'), *Lox* (5′-TGCGCTGCGGAAGAAAA-3′, 5′-TCTGACATCCGCCCTATATGC-3′), *Loxl1* (5′-CAGTGGATCGACATAACTGATGTG-3′, 5′-GGGTTCACGTGCACCTTGA-3′), *Loxl2* (5′-CCTCAAGGTTCCGGAAAGC-3′, 5′-ACCTCTCAGGCGCACCAA-3′), *Loxl3* (5′-TGTGCCTAGTCGAAGTGCC-3′, 5′-GTGTAGCAGCAGTAGTCCCC-3′), *Loxl4* (5′-TTGCTCTCAAGGACACCTGGTA-3′, 5′-GCAGCGAACTCCACTCATCA-3′), and *Gadph* (5'-TGCACCACCAACTGCTTAGC-3' and 5'-GGCATGGACTGTGGTCATGAG-3'). Target gene expression was estimated with the comparative $2^{-\Delta\Delta CT}$ method, using *Hprt1* or *Gadph* transcripts for normalization. Fold changes in normalized target gene expression were expressed relative to the mean values obtained from sham-operated mice, except for *Cnb1* mRNA expression, which is expressed as raw data.

4.8. Statistical analysis

All data are presented as means ± SEM (standard error of the mean). Statistical differences were analyzed with Graph-Pad Prism Version 7.03 (GraphPad, Inc., La Jolla, CA, USA). Data from different experimental groups were compared by one-way ANOVA followed by Tukey test, and the adjusted *P* values for multiples comparisons are indicated. Where indicated, comparisons between 2 groups were also made by unpaired, two-tailed Student *t* test. Differences were considered statistically significant at $P \leq 0.05$. The number of samples and independent experiments in each analysis are indicated in the corresponding figure legend.

ACKNOWLEDGMENTS

CNIC is supported by the Spanish Ministerio de Economía, Industria y Competitividad (MEIC) and the Pro-CNIC Foundation and is a Severo Ochoa Center of Excellence (MEIC award SEV-2015-0505). Support was also provided by grants from MEIC (SAF2012-34296 and SAF2015-636333R to J.M.R.), Fundació La Marató TV3 (20151330 to J.M.R.), Ministerio de Sanidad CIBERCV (CB16/11/00264 to J.M.R.), Comunidad de Madrid (AORTASANA-CM; B2017/BMD-3676 to JMR), and Red de Investigación Cardiovascular (RIC) (RD12/0042/0022 to J.M.R. and RD12/0042/0056 to J.L.J.-B.), and an FPU fellowship (AP 2009-1713 to N. L-V.)

We thank Dr. S. Bartlett for English language editing, Dr. Fátima Sánchez Cabo for statistical advice, Dr. M.R. Campanero, Dr. J. F. Nistal, and Dr. B. Ibañez for critical reading of the manuscript. We also thank Dr G. R. Crabtree for providing $Cnb1^{\Delta/flox}$ mice, A. Peral for technical assistance, and the ultrasonographers A.V. Alonso and L. Flores for technical support.

AUTHOR CONTRIBUTIONS

S. M-M., N. L-V. and MD. L-M. performed and designed the experiments, and acquired and analyzed the data. LJ. J-B., analyzed echocardiographic data. S. M-M., N. L-V., AL. A. and JM. R. wrote the manuscript. LJ. J-B and AL. A. made critical revision of the manuscript for key intellectual content. JM. R and SM-M designed and supervised the research.

Conflict of Interest

None declared

REFERENCES

1. Maillet, M., van Berlo, J. H. & Molkentin, J. D. (2013) Molecular basis of physiological heart growth: fundamental concepts and new players, *Nat Rev Mol Cell Biol.* **14**, 38-48.
2. Shimizu, I. & Minamino, T. (2016) Physiological and pathological cardiac hypertrophy, *J Mol Cell Cardiol.* **97**, 245-62.
3. van Berlo, J. H., Maillet, M. & Molkentin, J. D. (2013) Signaling effectors underlying pathologic growth and remodeling of the heart, *J Clin Invest.* **123**, 37-45.
4. Burchfield, J. S., Xie, M. & Hill, J. A. (2013) Pathological ventricular remodeling: mechanisms: part 1 of 2, *Circulation.* **128**, 388-400.
5. Molkentin, J. D. (2013) Parsing good versus bad signaling pathways in the heart: role of calcineurin-nuclear factor of activated T-cells, *Circ Res.* **113**, 16-9.
6. Berry, J. M., Le, V., Rotter, D., Battiprolu, P. K., Grinsfelder, B., Tannous, P., Burchfield, J. S., Czubryt, M., Backs, J., Olson, E. N., Rothermel, B. A. & Hill, J. A. (2011) Reversibility of adverse, calcineurin-dependent cardiac remodeling, *Circ Res.* **109**, 407-17.
7. Maillet, M., Davis, J., Auger-Messier, M., York, A., Osinska, H., Piquereau, J., Lorenz, J. N., Robbins, J., Ventura-Clapier, R. & Molkentin, J. D. (2010) Heart-specific deletion of CnB1 reveals multiple mechanisms whereby calcineurin regulates cardiac growth and function, *J Biol Chem.* **285**, 6716-24.
8. Schaeffer, P. J., Desantiago, J., Yang, J., Flagg, T. P., Kovacs, A., Weinheimer, C. J., Courtois, M., Leone, T. C., Nichols, C. G., Bers, D. M. & Kelly, D. P. (2009) Impaired contractile function and calcium handling in hearts of cardiac-specific calcineurin b1-deficient mice, *Am J Physiol Heart Circ Physiol.* **297**, H1263-73.
9. Li, M., Iismaa, S. E., Naqvi, N., Nicks, A., Husain, A. & Graham, R. M. (2014) Thyroid hormone action in postnatal heart development, *Stem Cell Res.* **13**, 582-91.
10. Nadruz, W. (2015) Myocardial remodeling in hypertension, *J Hum Hypertens.* **29**, 1-6.
11. Fabris, B., Candido, R., Bortoletto, M., Zentilin, L., Sandri, M., Fior, F., Toffoli, B., Stebel, M., Bardelli, M., Belgrado, D., Giacca, M. & Carretta, R. (2007) Dose and time-dependent apoptotic effects by angiotensin II infusion on left ventricular cardiomyocytes, *J Hypertens.* **25**, 1481-90.
12. Kurdi, M. & Booz, G. W. (2011) New take on the role of angiotensin II in cardiac hypertrophy and fibrosis, *Hypertension.* **57**, 1034-8.
13. Yagi, S., Aihara, K., Ikeda, Y., Sumitomo, Y., Yoshida, S., Ise, T., Iwase, T., Ishikawa, K., Azuma, H., Akaike, M. & Matsumoto, T. (2008) Pitavastatin, an HMG-CoA reductase inhibitor, exerts eNOS-independent protective actions against angiotensin II induced cardiovascular remodeling and renal insufficiency, *Circ Res.* **102**, 68-76.
14. Zhang, C., Li, Y., Wang, C., Wu, Y. & Du, J. (2014) Antagonist of C5aR prevents cardiac remodeling in angiotensin II-induced hypertension, *Am J Hypertens.* **27**, 857-64.
15. Di Marco, G. S., Reuter, S., Kentrup, D., Ting, L., Ting, L., Grabner, A., Jacobi, A. M., Pavenstadt, H., Baba, H. A., Tiemann, K. & Brand, M. (2011) Cardioprotective effect of calcineurin inhibition in an animal model of renal disease, *Eur Heart J.* **32**, 1935-45.
16. Murat, A., Pellieux, C., Brunner, H. R. & Pedrazzini, T. (2000) Calcineurin blockade prevents cardiac mitogen-activated protein kinase activation and hypertrophy in renovascular hypertension, *J Biol Chem.* **275**, 40867-73.
17. Takeda, Y., Yoneda, T., Demura, M., Usukura, M. & Mabuchi, H. (2002) Calcineurin inhibition attenuates mineralocorticoid-induced cardiac hypertrophy, *Circulation.* **105**, 677-9.
18. el Gamel, A., Keevil, B., Rahman, A., Campbell, C., Deiraniya, A. & Yonan, N. (1997) Cardiac allograft rejection: do trough cyclosporine levels correlate with the grade of histologic rejection?, *J Heart Lung Transplant.* **16**, 268-74.
19. Lim, H. W., De Windt, L. J., Steinberg, L., Taigen, T., Witt, S. A., Kimball, T. R. & Molkentin, J. D. (2000) Calcineurin expression, activation, and function in cardiac pressure-overload hypertrophy, *Circulation.* **101**, 2431-7.
20. Goldspink, P. H., McKinney, R. D., Kimball, V. A., Geenen, D. L. & Buttrick, P. M. (2001) Angiotensin II induced cardiac hypertrophy in vivo is inhibited by cyclosporin A in adult rats, *Mol Cell Biochem.* **226**, 83-8.
21. Davies, K. J., Ermak, G., Rothermel, B. A., Pritchard, M., Heitman, J., Ahnn, J., Henrique-Silva, F., Crawford, D., Canaider, S., Strippoli, P., Carinci, P., Min, K. T., Fox, D. S., Cunningham, K. W., Bassel-Duby, R., Olson, E. N., Zhang, Z., Williams, R. S., Gerber, H. P., Perez-Riba, M., Seo, H., Cao, X., Klee, C. B., Redondo, J. M., Maltais, L. J., Bruford, E. A., Povey, S., Molkentin, J. D., McKeon, F. D., Duh, E. J., Crabtree, G. R., Cyert, M. S., de la Luna, S. & Estivill, X. (2007) Renaming the DSCR1/Adapt78 gene family as RCAN: regulators of calcineurin, *FASEB J.* **21**, 3023-8.

22. Horsley, V. & Pavlath, G. K. (2002) NFAT: ubiquitous regulator of cell differentiation and adaptation, *J Cell Biol.* **156**, 771-4.
23. Hu, G., Wang, K., Groenendyk, J., Barakat, K., Mizianty, M. J., Ruan, J., Michalak, M. & Kurgan, L. (2014) Human structural proteome-wide characterization of Cyclosporine A targets, *Bioinformatics.* **30**, 3561-6.
24. Graef, I. A., Chen, F., Chen, L., Kuo, A. & Crabtree, G. R. (2001) Signals transduced by Ca(2+)/calcineurin and NFATc3/c4 pattern the developing vasculature, *Cell.* **105**, 863-75.
25. Neilson, J. R., Winslow, M. M., Hur, E. M. & Crabtree, G. R. (2004) Calcineurin B1 is essential for positive but not negative selection during thymocyte development, *Immunity.* **20**, 255-66.
26. Sohal, D. S., Nghiem, M., Crackower, M. A., Witt, S. A., Kimball, T. R., Tymitz, K. M., Penninger, J. M. & Molkentin, J. D. (2001) Temporally regulated and tissue-specific gene manipulations in the adult and embryonic heart using a tamoxifen-inducible Cre protein, *Circ Res.* **89**, 20-5.
27. Escolano, A., Martinez-Martinez, S., Alfranca, A., Urso, K., Izquierdo, H. M., Delgado, M., Martin, F., Sabio, G., Sancho, D., Gomez-del Arco, P. & Redondo, J. M. (2014) Specific calcineurin targeting in macrophages confers resistance to inflammation via MKP-1 and p38, *Embo J.* **33**, 1117-33.
28. Kong, P., Christia, P. & Frangogiannis, N. G. (2014) The pathogenesis of cardiac fibrosis, *Cell Mol Life Sci.* **71**, 549-74.
29. Flevaris, P., Khan, S. S., Eren, M., Schuldt, A. J. T., Shah, S. J., Lee, D. C., Gupta, S., Shapiro, A. D., Burridge, P. W., Ghosh, A. K. & Vaughan, D. E. (2017) Plasminogen Activator Inhibitor Type I Controls Cardiomyocyte Transforming Growth Factor-beta and Cardiac Fibrosis, *Circulation.* **136**, 664-679.
30. McCalmon, S. A., Desjardins, D. M., Ahmad, S., Davidoff, K. S., Snyder, C. M., Sato, K., Ohashi, K., Kielbasa, O. M., Mathew, M., Ewen, E. P., Walsh, K., Gavras, H. & Naya, F. J. (2010) Modulation of angiotensin II-mediated cardiac remodeling by the MEF2A target gene Xirp2, *Circ Res.* **106**, 952-60.
31. Bishop, J. E. & Laurent, G. J. (1995) Collagen turnover and its regulation in the normal and hypertrophying heart, *Eur Heart J.* **16 Suppl C**, 38-44.
32. Leask, A. (2015) Getting to the heart of the matter: new insights into cardiac fibrosis, *Circ Res.* **116**, 1269-76.
33. Lopez, B., Gonzalez, A., Hermida, N., Valencia, F., de Teresa, E. & Diez, J. (2010) Role of lysyl oxidase in myocardial fibrosis: from basic science to clinical aspects, *Am J Physiol Heart Circ Physiol.* **299**, H1-9.
34. Yang, J., Savvatis, K., Kang, J. S., Fan, P., Zhong, H., Schwartz, K., Barry, V., Mikels-Vigdal, A., Karpinski, S., Kornyeyev, D., Adamkewicz, J., Feng, X., Zhou, Q., Shang, C., Kumar, P., Phan, D., Kasner, M., Lopez, B., Diez, J., Wright, K. C., Kovacs, R. L., Chen, P. S., Quertermous, T., Smith, V., Yao, L., Tschope, C. & Chang, C. P. (2016) Targeting LOXL2 for cardiac interstitial fibrosis and heart failure treatment, *Nat Commun.* **7**, 13710.
35. Pellieux, C., Sauthier, T., Aubert, J. F., Brunner, H. R. & Pedrazzini, T. (2000) Angiotensin II-induced cardiac hypertrophy is associated with different mitogen-activated protein kinase activation in normotensive and hypertensive mice, *J Hypertens.* **18**, 1307-17.
36. Bourajjaj, M., Armand, A. S., da Costa Martins, P. A., Weijts, B., van der Nagel, R., Heeneman, S., Wehrens, X. H. & De Windt, L. J. (2008) NFATc2 is a necessary mediator of calcineurin-dependent cardiac hypertrophy and heart failure, *J Biol Chem.* **283**, 22295-303.
37. Bueno, O. F., Wilkins, B. J., Tymitz, K. M., Glascock, B. J., Kimball, T. F., Lorenz, J. N. & Molkentin, J. D. (2002) Impaired cardiac hypertrophic response in Calcineurin Abeta -deficient mice, *Proc Natl Acad Sci U S A.* **99**, 4586-91.
38. Wilkins, B. J., De Windt, L. J., Bueno, O. F., Braz, J. C., Glascock, B. J., Kimball, T. F. & Molkentin, J. D. (2002) Targeted disruption of NFATc3, but not NFATc4, reveals an intrinsic defect in calcineurin-mediated cardiac hypertrophic growth, *Mol Cell Biol.* **22**, 7603-13.
39. Brand, S., Amann, K. & Schupp, N. (2013) Angiotensin II-induced hypertension dose-dependently leads to oxidative stress and DNA damage in mouse kidneys and hearts, *J Hypertens.* **31**, 333-44.
40. Capone, C., Faraco, G., Park, L., Cao, X., Davisson, R. L. & Iadecola, C. (2011) The cerebrovascular dysfunction induced by slow pressor doses of angiotensin II precedes the development of hypertension, *Am J Physiol Heart Circ Physiol.* **300**, H397-407.
41. Kawada, N., Imai, E., Karber, A., Welch, W. J. & Wilcox, C. S. (2002) A mouse model of angiotensin II slow pressor response: role of oxidative stress, *J Am Soc Nephrol.* **13**, 2860-8.
42. Welch, W. J., Chabrashvili, T., Solis, G., Chen, Y., Gill, P. S., Aslam, S., Wang, X., Ji, H., Sandberg, K., Jose, P. & Wilcox, C. S. (2006) Role of extracellular superoxide dismutase in the mouse angiotensin slow pressor response, *Hypertension.* **48**, 934-41.

43. Parra, V. & Rothermel, B. A. (2016) Calcineurin signaling in the heart: The importance of time and place, *J Mol Cell Cardiol*.
44. Hill, J. A., Rothermel, B., Yoo, K. D., Cabuay, B., Demetroulis, E., Weiss, R. M., Kutschke, W., Bassel-Duby, R. & Williams, R. S. (2002) Targeted inhibition of calcineurin in pressure-overload cardiac hypertrophy. Preservation of systolic function, *J Biol Chem.* **277**, 10251-5.
45. Wilkins, B. J. & Molkentin, J. D. (2004) Calcium-calcineurin signaling in the regulation of cardiac hypertrophy, *Biochem Biophys Res Commun.* **322**, 1178-91.
46. Yang, G., Meguro, T., Hong, C., Asai, K., Takagi, G., Karoor, V. L., Sadoshima, J., Vatner, D. E., Bishop, S. P. & Vatner, S. F. (2001) Cyclosporine reduces left ventricular mass with chronic aortic banding in mice, which could be due to apoptosis and fibrosis, *J Mol Cell Cardiol.* **33**, 1505-14.
47. Bianchi, R., Rodella, L. & Rezzani, R. (2003) Cyclosporine A up-regulates expression of matrix metalloproteinase 2 and vascular endothelial growth factor in rat heart, *Int Immunopharmacol.* **3**, 427-33.
48. Djamali, A., Reese, S., Hafez, O., Vidyasagar, A., Jacobson, L., Swain, W., Kolehmainen, C., Huang, L., Wilson, N. A. & Torrealba, J. R. (2012) Nox2 is a mediator of chronic CsA nephrotoxicity, *Am J Transplant.* **12**, 1997-2007.
49. Minguillon, J., Morancho, B., Kim, S. J., Lopez-Botet, M. & Aramburu, J. (2005) Concentrations of cyclosporin A and FK506 that inhibit IL-2 induction in human T cells do not affect TGF-beta1 biosynthesis, whereas higher doses of cyclosporin A trigger apoptosis and release of preformed TGF-beta1, *J Leukoc Biol.* **77**, 748-58.
50. Hong, F., Lee, J., Song, J. W., Lee, S. J., Ahn, H., Cho, J. J., Ha, J. & Kim, S. S. (2002) Cyclosporin A blocks muscle differentiation by inducing oxidative stress and inhibiting the peptidyl-prolyl-cis-trans isomerase activity of cyclophilin A: cyclophilin A protects myoblasts from cyclosporin A-induced cytotoxicity, *FASEB J.* **16**, 1633-5.
51. Chen, J., Yang, F., Yu, X., Yu, Y. & Gong, Y. (2016) Cyclosporine A promotes cell proliferation, collagen and alpha-smooth muscle actin expressions in rat gingival fibroblasts by Smad3 activation and miR-29b suppression, *J Periodontal Res.* **51**, 735-747.
52. Mohamed, M. A., Robertson, H., Booth, T. A., Balupuri, S., Kirby, J. A. & Talbot, D. (2000) TGF-beta expression in renal transplant biopsies: a comparative study between cyclosporin-A and tacrolimus, *Transplantation.* **69**, 1002-5.
53. Wolf, G., Thaiss, F. & Stahl, R. A. (1995) Cyclosporine stimulates expression of transforming growth factor-beta in renal cells. Possible mechanism of cyclosporines antiproliferative effects, *Transplantation.* **60**, 237-41.
54. Fraser, D. J., Phillips, A. O., Zhang, X., van Roeyen, C. R., Muehlenberg, P., En-Nia, A. & Mertens, P. R. (2008) Y-box protein-1 controls transforming growth factor-beta1 translation in proximal tubular cells, *Kidney Int.* **73**, 724-32.
55. Hanssen, L., Frye, B. C., Ostendorf, T., Alidousty, C., Djudjaj, S., Boor, P., Rauen, T., Floege, J., Mertens, P. R. & Raffetseder, U. (2011) Y-box binding protein-1 mediates profibrotic effects of calcineurin inhibitors in the kidney, *J Immunol.* **187**, 298-308.
56. Kakkar, R. & Lee, R. T. (2010) Intramyocardial fibroblast myocyte communication, *Circ Res.* **106**, 47-57.
57. Kung, L., Batiuk, T. D., Palomo-Pinon, S., Noujaim, J., Helms, L. M. & Halloran, P. F. (2001) Tissue distribution of calcineurin and its sensitivity to inhibition by cyclosporine, *Am J Transplant.* **1**, 325-33.
58. Travers, J. G., Kamal, F. A., Robbins, J., Yutzey, K. E. & Blaxall, B. C. (2016) Cardiac Fibrosis: The Fibroblast Awakens, *Circ Res.* **118**, 1021-40.
59. Heymans, S., Gonzalez, A., Pizard, A., Papageorgiou, A. P., Lopez-Andres, N., Jaisser, F., Thum, T., Zannad, F. & Diez, J. (2015) Searching for new mechanisms of myocardial fibrosis with diagnostic and/or therapeutic potential, *Eur J Heart Fail.* **17**, 764-71.
60. Galan, M., Varona, S., Guadall, A., Orriols, M., Navas, M., Aguilo, S., de Diego, A., Navarro, M. A., Garcia-Dorado, D., Rodriguez-Sinovas, A., Martinez-Gonzalez, J. & Rodriguez, C. (2017) Lysyl oxidase overexpression accelerates cardiac remodeling and aggravates angiotensin II-induced hypertrophy, *FASEB J.* **31**, 3787-3799.
61. Gonzalez-Santamaria, J., Villalba, M., Busnadiego, O., Lopez-Olaneta, M. M., Sandoval, P., Snabel, J., Lopez-Cabrera, M., Erler, J. T., Hanemaaijer, R., Lara-Pezzi, E. & Rodriguez-Pascual, F. (2016) Matrix cross-linking lysyl oxidases are induced in response to myocardial infarction and promote cardiac dysfunction, *Cardiovasc Res.* **109**, 67-78.
62. Hermida, N., Lopez, B., Gonzalez, A., Dotor, J., Lasarte, J. J., Sarobe, P., Borras-Cuesta, F. & Diez, J. (2009) A synthetic peptide from transforming growth factor-beta1 type III receptor prevents myocardial fibrosis in spontaneously hypertensive rats, *Cardiovasc Res.* **81**, 601-9.

63. Ohmura, H., Yasukawa, H., Minami, T., Sugi, Y., Oba, T., Nagata, T., Kyogoku, S., Ohshima, H., Aoki, H. & Imaizumi, T. (2012) Cardiomyocyte-specific transgenic expression of lysyl oxidase-like protein-1 induces cardiac hypertrophy in mice, *Hypertens Res.* **35**, 1063-8.
64. Busnadiego, O., Gonzalez-Santamaria, J., Lagares, D., Guinea-Viniegra, J., Pichol-Thievend, C., Muller, L. & Rodriguez-Pascual, F. (2013) LOXL4 is induced by transforming growth factor beta1 through Smad and JunB/Fra2 and contributes to vascular matrix remodeling, *Mol Cell Biol.* **33**, 2388-401.
65. Sethi, A., Mao, W., Wordinger, R. J. & Clark, A. F. (2011) Transforming growth factor-beta induces extracellular matrix protein cross-linking lysyl oxidase (LOX) genes in human trabecular meshwork cells, *Invest Ophthalmol Vis Sci.* **52**, 5240-50.
66. Voloshenyuk, T. G., Landesman, E. S., Khoutorova, E., Hart, A. D. & Gardner, J. D. (2011) Induction of cardiac fibroblast lysyl oxidase by TGF-beta1 requires PI3K/Akt, Smad3, and MAPK signaling, *Cytokine.* **55**, 90-7.
67. Indra, A. K., Warot, X., Brocard, J., Bornert, J. M., Xiao, J. H., Chambon, P. & Metzger, D. (1999) Temporally-controlled site-specific mutagenesis in the basal layer of the epidermis: comparison of the recombinase activity of the tamoxifen-inducible Cre-ER(T) and Cre-ER(T2) recombinases, *Nucleic Acids Res.* **27**, 4324-7.
68. Dai, W., He, W., Shang, G., Jiang, J., Wang, Y. & Kong, W. (2010) Gene silencing of myofibrillogenesis regulator-1 by adenovirus-delivered small interfering RNA suppresses cardiac hypertrophy induced by angiotensin II in mice, *Am J Physiol Heart Circ Physiol.* **299**, H1468-75.
69. Schneider, C. A., Rasband, W. S. & Eliceiri, K. W. (2012) NIH Image to ImageJ: 25 years of image analysis, *Nat Methods.* **9**, 671-5.
70. Graumann, J., Hubner, N. C., Kim, J. B., Ko, K., Moser, M., Kumar, C., Cox, J., Scholer, H. & Mann, M. (2008) Stable isotope labeling by amino acids in cell culture (SILAC) and proteome quantitation of mouse embryonic stem cells to a depth of 5,111 proteins, *Mol Cell Proteomics.* **7**, 672-83.

FIGURE LEGENDS

Fig. 1. Cn inhibition by CsA attenuates cardiac hypertrophy induced by pressor doses of AngII. Wild type mice were minipump-infused with AngII (60 μg/kg/h) in the presence (CsA/AngII) or absence of CsA (0.208 mg/kg/h) for 21 days. Control mice underwent surgery without minipump implantation (sham). **(A)** Ratios of ventricular weight to body weight (VW/BW) and ventricular weight to tibial length (VW/TL). Symbols represent data from individual mice; horizontal lines show means ± SEM (n=7-17 mice/group, 3 independent experiments). **(B)** Analysis of cardiomyocyte cross-sectional area on cardiac histological sections stained with FITC-*T. vulgaris* lectin. Images show representative microscopy fields. Scale bar, 50 μm. The histogram shows individual data and means ± SEM (n=7-19 mice/group, 4 independent experiments). Data in A and B were analyzed by one-way ANOVA with a post hoc Tukey comparison test, the adjusted *P* values are shown.

Fig. 2. AngII induces the early appearance of a Cn-dependent cardiac hypertrophic phenotype. (A) qPCR analysis of *Rcan1.4* and *Ptgs-2* gene expression in the hearts of mice treated with AngII (60 μg/kg/h) as indicated. Results are expressed as fold-increase relative to control animals (sham). Data are means ± SEM (n=2-3 mice/group). **(B)** Western blot analysis of Rcan1.4 protein expression in the hearts of mice treated with AngII (60 μg/kg/h) for 1 day in the presence or absence of CsA (0.208 mg/kg/h). Expression of α-Tubulin (α-Tub) was determined as a loading control. The presented blot is representative of 3 experiments. **(C)** Western blot analysis of Rcan1.4 and Cox-2 protein expression in heart protein lysates from wild-type mice infused for 1 or 2 days with AngII (60 μg/kg/h) in the presence or absence of CsA (0.832 mg/kg/h). Levels of α-Actinin (α-Act) were determined as a loading control **(D-F)** Analysis of cardiac hypertrophy in mice treated as indicated for 1 or 3 days. **(D)** Ratios of ventricular weight to body weight (VW/BW) and ventricular weight to tibia length (VW/TL). **(E)** Cardiomyocyte cross-sectional area. **(F)** Interventricular septum wall thickness. Histograms show individual data and means ± SEM (n=12-14 mice/group, 3 independent experiments in D and n=9-12 mice/group, 2 independent experiments in E and F). All data were analyzed by one-way ANOVA with a post hoc Tukey comparison test, the adjusted *P* values are shown. Parameters in D were compared by unpaired, two-tailed Student *t* test; $^{*}P$.

Fig. 3. Cardiac *Cnb1* deletion reduces AngII-induced *Rcan1.4* and *Ptgs2* expression in the heart. (A) Western blot analysis of calcineurin subunit A (CnA) and subunit B (CnB) expression in the hearts of Cnb1-flox^{Myh6} mice after treatment with vehicle (Veh) or 4-hydroxy tamoxifen (Tx). Expression of α-Tubulin (α-Tub) was determined as a loading control. (**B**) Western blot analysis of CnB expression in protein lysates from thymus, aorta, kidney, and liver Cnb1-flox^{Myh6} mice treated with vehicle (Veh) or 4-hydroxy tamoxifen (Tx). α-Tubulin (α-Tub) was analyzed as a loading control. **(C)** qPCR analysis of *Rcan1.4* and *Ptgs2* mRNA expression in Cnb1-flox^{Myh6} mice treated with 4-hydroxy tamoxifen (Tx) or vehicle (Veh) and subsequently infused with AngII for 1 day. Data are means ± SEM (n=2-7 mice/group), and were analyzed by one-way ANOVA with a post-hoc Tukey

comparison test, the adjusted *P* values are shown **(D)** Western blot analysis of Rcan1.4 protein expression in Cnb1-flox^{Myh6} mice treated with AngII for 1 day. α-Tubulin (α-Tub) was analyzed as loading control.

Fig. 4. Specific deletion of Cn in the adult heart impairs AngII-mediated cardiac hypertrophy. **(A)** Ratios of ventricular weight to body weight (VW/BW) and ventricular weight to tibia length (VW/TL) in Cnb1-flox^{Myh6} mice treated with vehicle or Tx and subsequently infused with AngII or CsA plus AngII (CsA/AngII) for 21 days. **(B)** Cardiomyocyte cross-sectional area in mice treated as in A. Histograms in A and B show individual data and means ± SEM (n=10-20 mice/group, ≥3 independent experiments). Images show representative cardiac cross-sectional microscopy fields quantified in the histogram. Scale bar, 50 μm. Data were analyzed by one-way ANOVA with a post hoc Tukey comparison test.

Fig. 5. Expression of cardiac Cn is required for AngII-induced fibrosis in the heart. (A-B) Picrosirius Red staining of collagen on histological sections of hearts isolated from wild type mice infused for 21 days (A) or 1 and 3 days (B) with AngII (60 μg/kg/h) in the presence or absence of CsA (0.208 mg/kg/h). Histograms show individual data and means ± SEM (n=8-15 mice/group, ≥2 independent experiments). Images show representative staining in experiments quantified in the histogram in A. Scale bar, 1 mm. **(C)** qPCR analysis of *Col3a1* RNA in the hearts of wild-type mice treated as above for 1 and 3 days. Data are means ± SEM (n=7-13 mice/group, 2 independent experiments). **(D)** Picrosirius Red staining of collagen on histological sections of hearts isolated from Cnb1-flox^{Myh6} mice treated with vehicle (Veh) or 4-hydroxy tamoxifen (Tx) and subsequently infused with AngII for 21 days. When indicated, AngII-infused animals were co-treated with CsA. Images show representative staining in experiments quantified in the histogram. Scale bar, 1 mm. The histogram shows individual data and means ± SEM (n=11-14 mice/group, 3 independent experiments). All data were analyzed by one-way ANOVA with a post hoc Tukey comparison test. Parameters in B were compared by unpaired, two-tailed Student *t* test; $^{*}P$.

Fig. 6. Cardiac *Cnb1* deletion attenuates CH and fibrosis at the onset of the disease. Cnb1-flox^{Myh6} mice were treated with vehicle (Veh) or 4-hydroxy tamoxifen (Tx) and subsequently infused with AngII for 3 days. **(A)** Ventricular weight to body weight (VW/BW) ratio. **(B)** Ventricular weight to tibia length (VW/TL) ratio. **(C)** Interventricular septum wall thickness. **(D)** Cardiac fibrosis, measured as Picrosirius Red collagen staining on histological sections. Data are means ± SEM (n=7-15 mice/group, 2 or 3 independent experiments). Data were analyzed by one-way ANOVA with a post hoc Tukey comparison test, the adjusted *P* values are shown. For VW/TL ratios, comparisons between 2 groups were made by unpaired, two-tailed Student *t* test; $^{*}P$.

Fig. 7. Cardiac *Cnb1* deletion reduces AngII-induced apoptosis in the heart. TUNEL assays on histological sections of hearts isolated from **(A)** wild type mice infused for 3 days with AngII (60 μg/kg/h) in the presence or absence of CsA (0.208 mg/kg/h) or **(B)** from Cnb1-flox^{Myh6} mice treated with vehicle (Veh) or 4-hydroxy tamoxifen (Tx) and subsequently infused with AngII for 3 days**.** Histograms show individual data and means ±

SEM (n=4 mice/group). Images show representative staining in each group. Scale bar, 50 μm. All data were analyzed by one-way ANOVA with a post hoc Tukey comparison test. Nuclei from apoptotic cells are stained in brown/black.

Fig. 8. Cardiac Cn expression is essential for the expression of specific pro-fibrotic genes. (A) qPCR analysis of pro-fibrotic genes in the heart of wild-type mice after infusion with AngII for 1 and 3 days. Data are means ± SEM, n=4-6 mice/time point and were analysed by one-way ANOVA with a post hoc Tukey comparison test; the adjusted *P* values are shown; $^{*}P$ value was acquired by unpaired, two-tailed Student *t* test. **(B)** qPCR analysis of pro-fibrotic genes in the hearts of CsA-treated wild-type mice (left) or Tx-treated Cnb1-flox^{Myh6} mice (right) after AngII infusion for the optimal period for each gene, obtained from results in A (1 day after AngII infusion except for *Tgfβ3,* which was analyzed 3 days after AngII infusion). Data are means ± SEM (n=4-6 mice/group for *Il6* and *Tgfβ3*; n=7-14 mice/group for *Tgfβ1, Tgfβ2*, and *Tgfβi*). **(C)** qPCR analysis of collagen genes in the hearts of CsA-treated wild-type mice (left) or Tx-treated Cnb1-flox^{Myh6} mice (right) after AngII infusion for 3 days. Data are means ± SEM (n=5-8 mice/group). **(D)** qPCR analysis of *Lox* in the hearts of CsA-treated wild-type mice (left) or Tx-treated Cnb1-flox^{Myh6} mice (right) after AngII infusion for 1 day. Data are means ± SEM (n=8-14 mice/group). Data in B-D were obtained from 3 independent experiments, and were analyzed by one-way ANOVA with a post Tukey comparison test, $^{*}P$ value was acquired by unpaired, two-tailed Student *t* test **(E)** Western blot analysis of Lox protein expression in cardiac protein lysates isolated from the experimental mouse models described above after AngII infusion for 3 days. Levels of α-Tubulin (α-Tub) were determined as a loading control; n=3-5 mice/group. Arrows indicate the specific Lox protein band.

Fig. 9. AngII-induced expression of *Loxl*4 is selectively affected by cardiac-specific Cn deletion. qPCR analysis of *Loxl* genes (*Loxl1, Loxl2, Loxl3 and Loxl4*) in the hearts of CsA-treated wild-type mice (left) and Tx-treated Cnb1-flox^{Myh6} mice (right) after AngII infusion for 1 day. Data are means ± SEM (n=6-14 mice/group), and were analyzed by one-way ANOVA with a post hoc Tukey comparison test, the adjusted *P* values are shown For *Loxl3* expression in wild-type mice, comparisons between 2 groups were made by unpaired, two-tailed Student *t* test; $^{*}P$.

Table 1. Effect of a pharmacological CsA concentration (0.208 mg/kg/h) on echocardiographic parameters and systolic blood pressure determined in wild-type control (sham-implanted) mice or mice infused with AngII (60 µg/kg/h) for 21 days.

	sham	AngII	CsA	CsA/AngII
Heart rate (bpm)	488 ± 15	515 ± 13	528 ± 21	499 ± 19
IVS, d (mm)	0.76 ± 0.02	0.94 ± 0.03 ($^{\#}P$<0.0001)	0.78 ± 0.02	0.85 ± 0.02 ($^{\dagger}P$=0.0398)
LVPW, d (mm)	0.75 ± 0.02	0.85± 0.03 ($^{\#}P$=0.0277)	0.70 ± 0.01	0.79 ± 0.03
LVID, d (mm)	3.88 ± 0.06	3.75 ± 0.09	3.86 ± 0.08	3.79 ± 0.07
EF (%)	52.5 ± 1.6	50.7 ± 2.3	49.9 ± 2.2	45.8 ± 2.3
Systolic BP (mmHg**)**	109.7 ± 3.0	145.1 ± 6.7 ($^{\#}P$<0.0001)	113.4 ± 1.9	143.5 ± 4.1 ($^{\#}P$<0.0001)

IVS d, diastolic interventricular septum thickness; LVPW d, diastolic left ventricular posterior wall thickness; LVID d, diastolic left ventricle internal diameter; EF, ejection fraction; SBP, systolic blood pressure; bpm, beats per minute.

Data are means ± SEM (n=9-15 mice/group, from 3 independent experiments), and were analyzed by one-way ANOVA with a post hoc Tukey comparison test; and the adjusted *P* values are shown: $^{\#}P$ *vs* sham group; $^{\dagger}P$ *vs* AngII group

Table 2. Echocardiographic parameters in Cnb1-flox^{Myh6} mice treated with vehicle or 4-hydroxy tamoxifen (Tx) and subsequently infused with AngII for 21 days.

	sham	AngII	Tx/sham	Tx/AngII
Heart rate (bpm)	504 ± 24	574 ± 14	542 ± 26	511 ± 17
IVS, d (mm)	0.73 ± 0.02	0.94 ± 0.04 ($^{\#}P$<0.0001)	0.74 ± 0.02	0.84 ± 0.03
LVPW, d (mm)	0.71 ± 0.02	0.96 ± 0.03 ($^{\#}P$<0.0001)	0.80 ± 0.03	0.85 ± 0.02 ($^{\dagger}P$=0.0252)
LVID, d (mm)	3.72 ± 0.10	3.35 ± 0.16	3.54 ± 0.11	3.38 ± 0.09
EF (%)	48.7 ± 2.0	56.3 ± 2.2	61.8± 2.4 ($^{\#}P$=0.0013)	52.3 ± 2.7

IVS d, diastolic interventricular septum thickness; LVPW d, diastolic left ventricular posterior wall thickness; LVID d, diastolic left ventricle internal diameter; EF, ejection fraction; bpm, beats per minute.

Data are means ± SEM (n=8-10 mice/group, 2 independent experiments), and were analyzed by one-way ANOVA with a post hoc Tukey comparison test; and the adjusted *P* values are shown: $^{\#}P$ *vs* sham group; $^{\dagger}P$ *vs* AngII group.

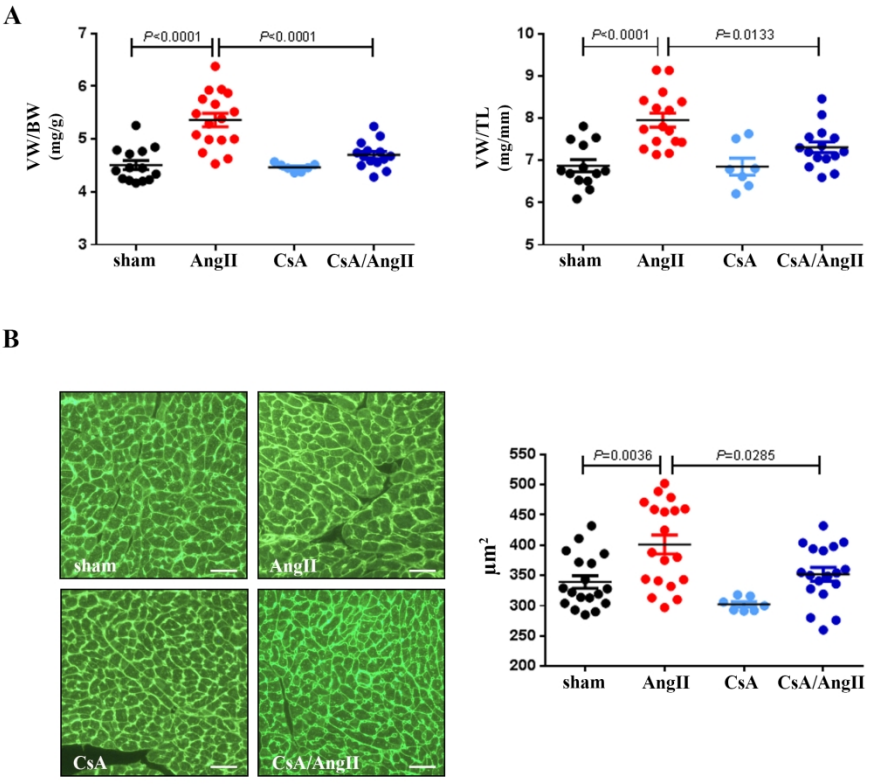
A
P<0.0001
P<0.0001
VW/BW (mg/g)
sham
AngII
CsA
CsA/AngII
P<0.0001
P=0.0133
VW/TL (mg/mm)
B
sham
AngII
CsA
CsA/AngII
P=0.0036
P=0.0285
μm²

FIGURE 1

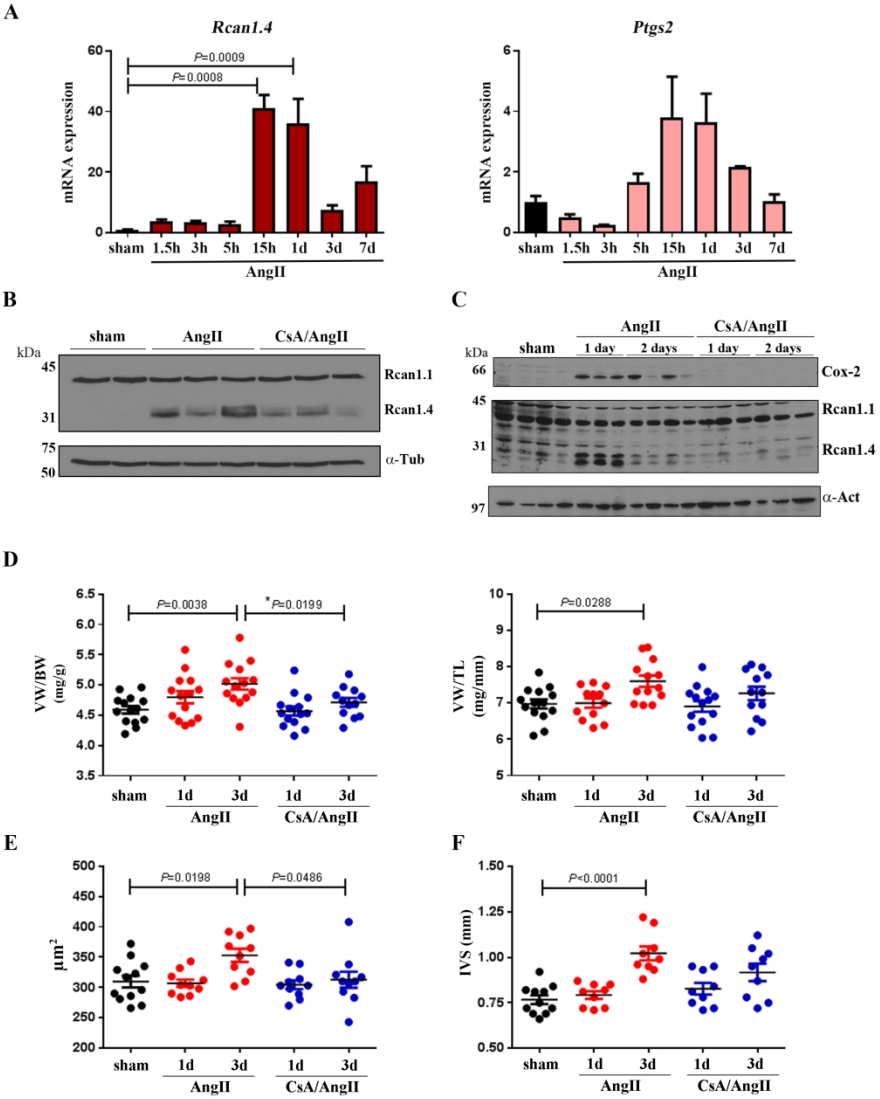
A
Rcan1.4
P=0.0009
P=0.0008
mRNA expression
sham 1.5h 3h 5h 15h 1d 3d 7d
AngII
Ptgs2
mRNA expression
sham 1.5h 3h 5h 15h 1d 3d 7d
AngII
B
sham
AngII
CsA/AngII
kDa
45
31
75
50
Rcan1.1
Rcan1.4
α-Tub
C
AngII
CsA/AngII
sham
1 day
2 days
1 day
2 days
kDa
66
45
31
97
Cox-2
Rcan1.1
Rcan1.4
α-Act
D
P=0.0038
*P=0.0199
VW/BW (mg/g)
sham 1d 3d 1d 3d
AngII
CsA/AngII
P=0.0288
VW/TL (mg/mm)
sham 1d 3d 1d 3d
AngII
CsA/AngII
E
P=0.0198
P=0.0486
μm²
sham 1d 3d 1d 3d
AngII
CsA/AngII
F
P<0.0001
IVS (mm)
sham 1d 3d 1d 3d
AngII
CsA/AngII

FIGURE 2

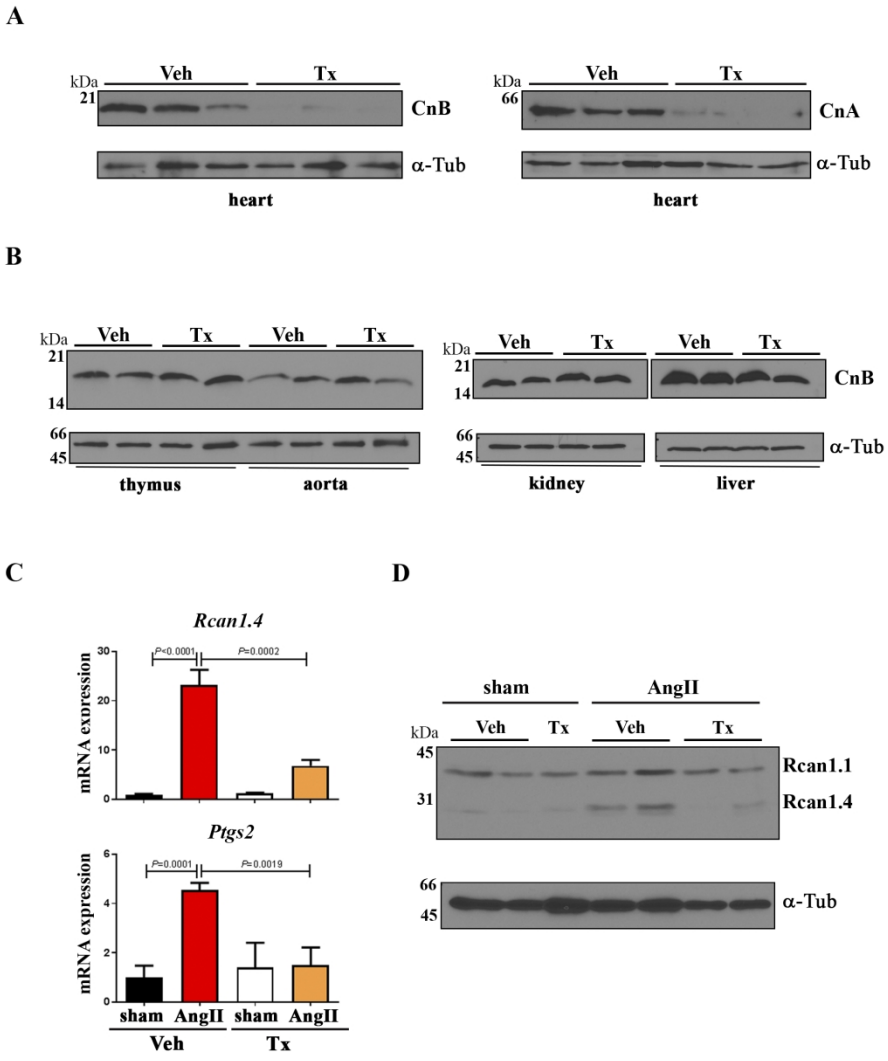
A
kDa
Veh
Tx
21
CnB
α-Tub
heart
kDa
Veh
Tx
66
CnA
α-Tub
heart
B
kDa
Veh
Tx
Veh
Tx
21
14
66
45
thymus
aorta
kDa
Veh
Tx
Veh
Tx
21
14
CnB
66
45
α-Tub
kidney
liver
C
Rcan1.4
mRNA expression
P<0.0001
P=0.0002
30
20
10
0
Ptgs2
mRNA expression
P=0.0001
P=0.0019
6
4
2
0
sham
AngII
sham
AngII
Veh
Tx
D
sham
AngII
kDa
Veh
Tx
Veh
Tx
45
31
Rcan1.1
Rcan1.4
66
45
α-Tub

FIGURE 3

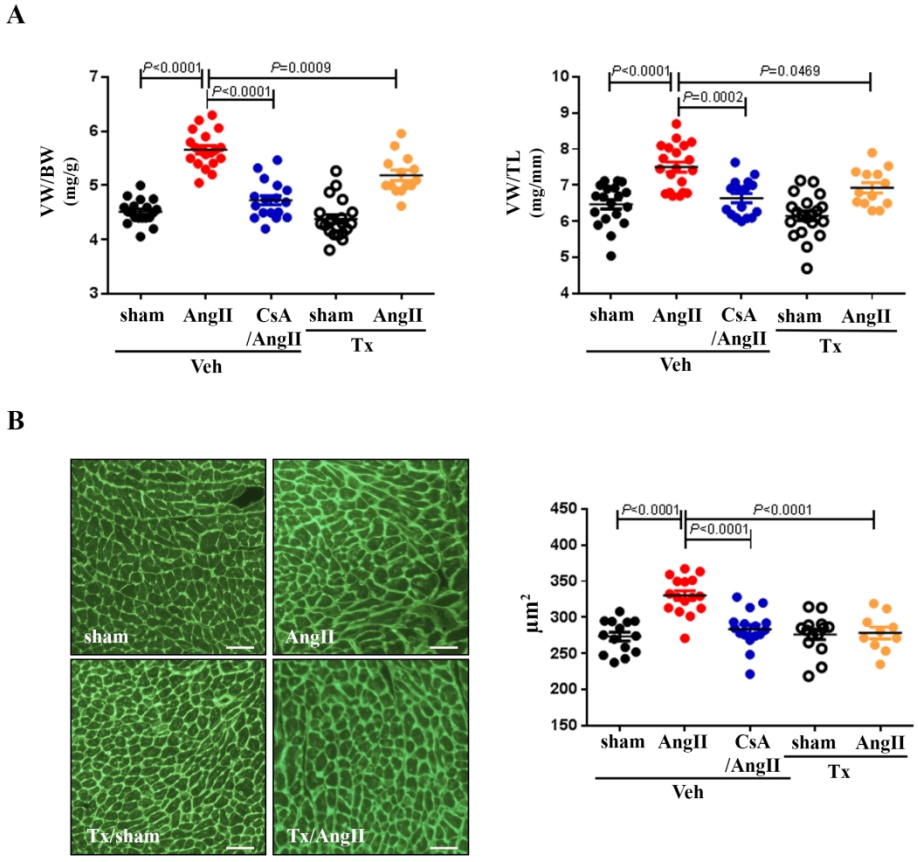
A
P<0.0001
P=0.0009
P<0.0001
VW/BW (mg/g)
sham
AngII
CsA /AngII
sham
AngII
Veh
Tx
P<0.0001
P=0.0469
P=0.0002
VW/TL (mg/mm)
B
sham
AngII
Tx/sham
Tx/AngII
P<0.0001
P<0.0001
P<0.0001
μm²

FIGURE 4

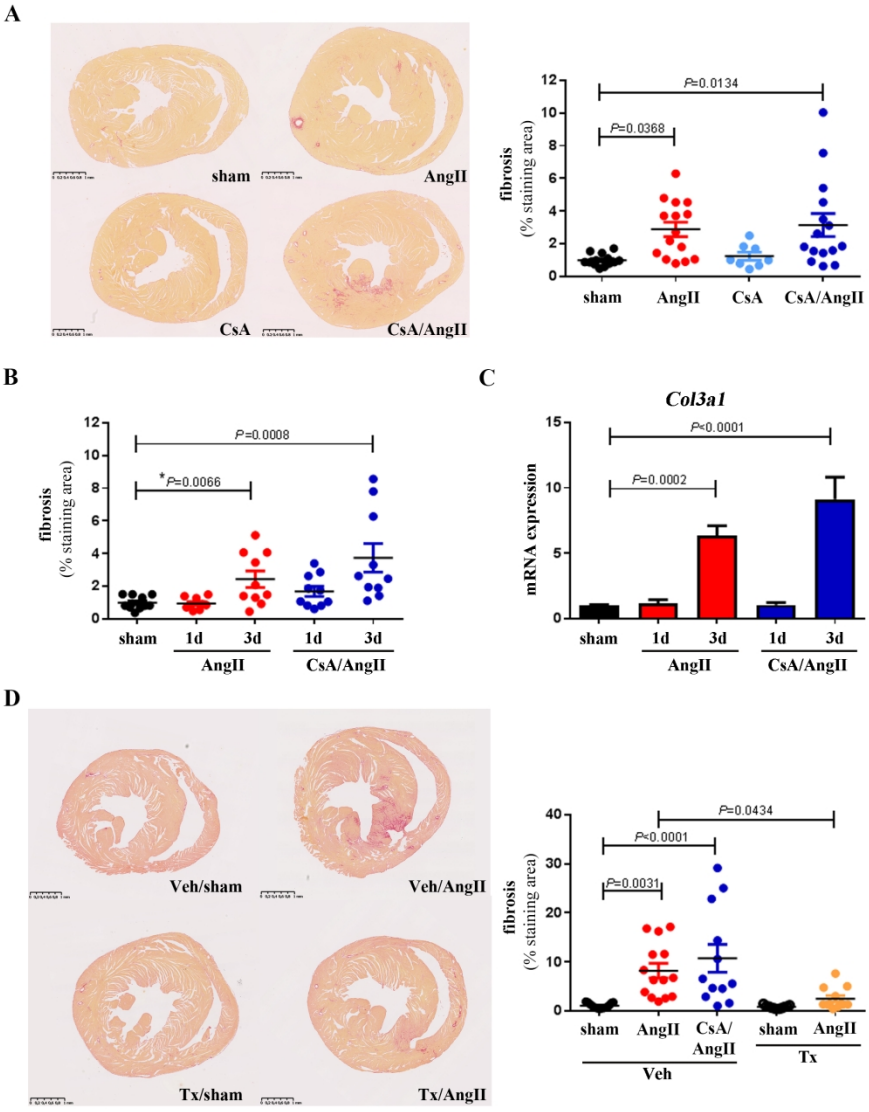
A
sham
AngII
CsA
CsA/AngII
fibrosis (% staining area)
P=0.0134
P=0.0368
sham
AngII
CsA
CsA/AngII
B
fibrosis (% staining area)
P=0.0008
*P=0.0066
sham
1d
3d
1d
3d
AngII
CsA/AngII
C
Col3a1
mRNA expression
P<0.0001
P=0.0002
sham
1d
3d
1d
3d
AngII
CsA/AngII
D
Veh/sham
Veh/AngII
Tx/sham
Tx/AngII
fibrosis (% staining area)
P=0.0434
P<0.0001
P=0.0031
sham
AngII
CsA/ AngII
sham
AngII
Veh
Tx

FIGURE 5

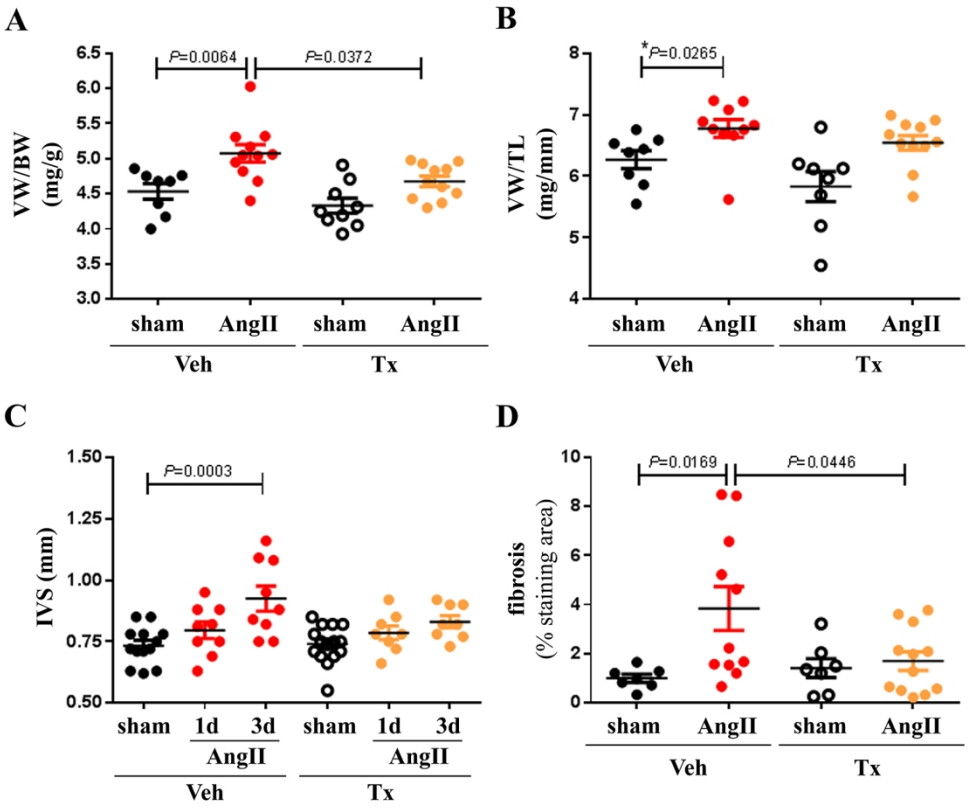
A
VW/BW (mg/g)
P=0.0064
P=0.0372
sham
AngII
sham
AngII
Veh
Tx
B
VW/TL (mg/mm)
*P=0.0265
sham
AngII
sham
AngII
Veh
Tx
C
IVS (mm)
P=0.0003
sham
1d
3d
AngII
sham
1d
3d
AngII
Veh
Tx
D
fibrosis (% staining area)
P=0.0169
P=0.0446
sham
AngII
sham
AngII
Veh
Tx

FIGURE 6

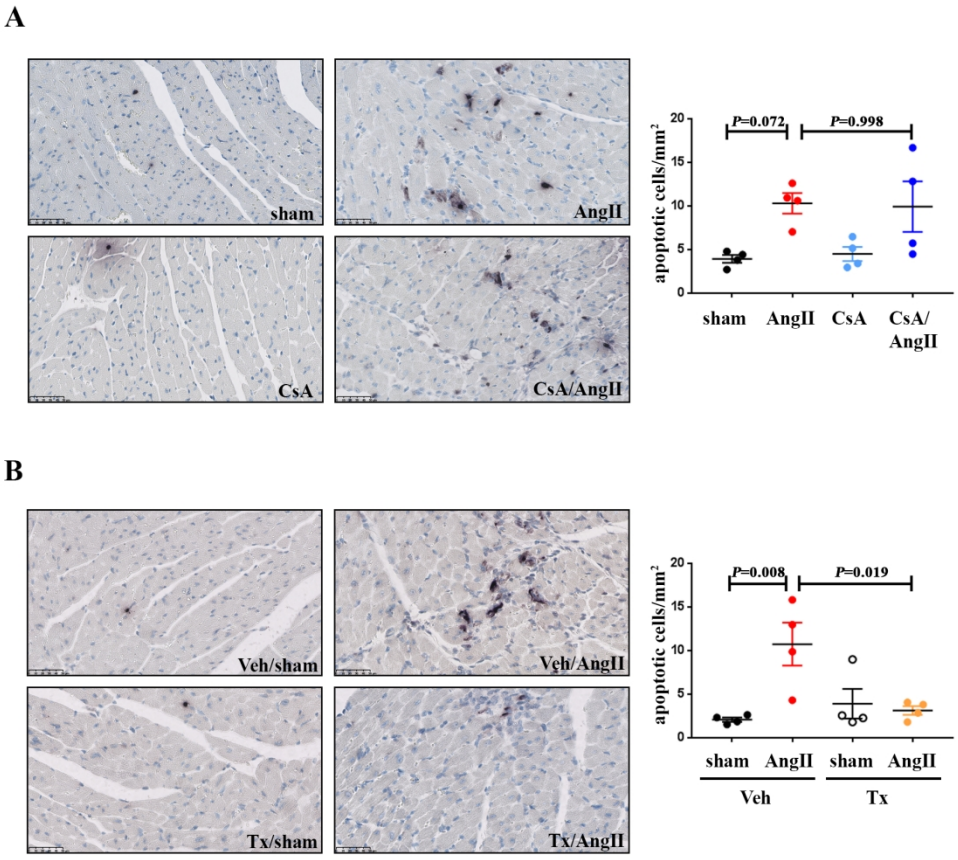
A
sham
AngII
CsA
CsA/AngII
P=0.072
P=0.998
apoptotic cells/mm²
sham
AngII
CsA
CsA/ AngII
B
Veh/sham
Veh/AngII
Tx/sham
Tx/AngII
P=0.008
P=0.019
apoptotic cells/mm²
sham
AngII
sham
AngII
Veh
Tx

FIGURE 7

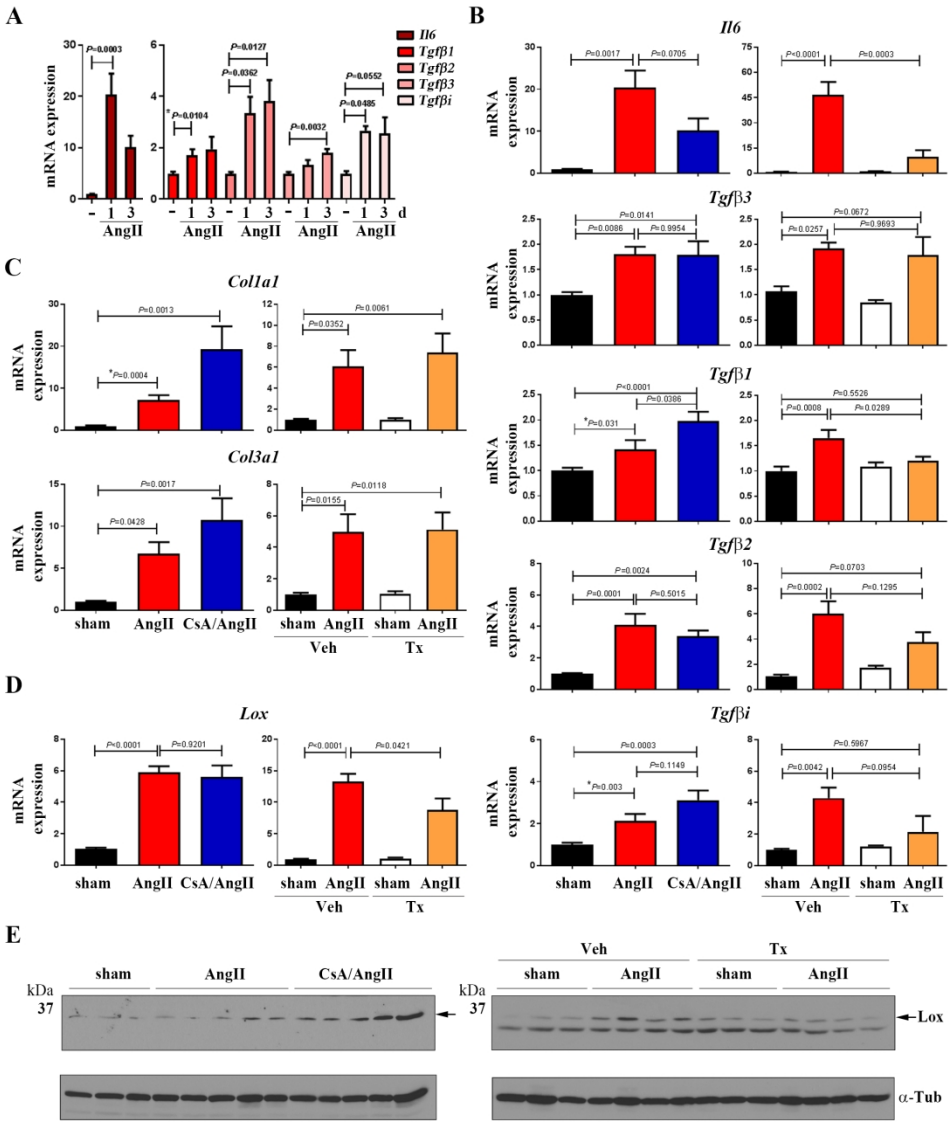
A
B
C
D
E
Il6
Tgfβ1
Tgfβ2
Tgfβ3
Tgfβi
mRNA expression
AngII
Col1a1
Col3a1
Tgfβ3
Tgfβ1
Tgfβ2
Lox
Tgfβi
sham
AngII
CsA/AngII
Veh
Tx
kDa
37
Lox
α-Tub

FIGURE 8

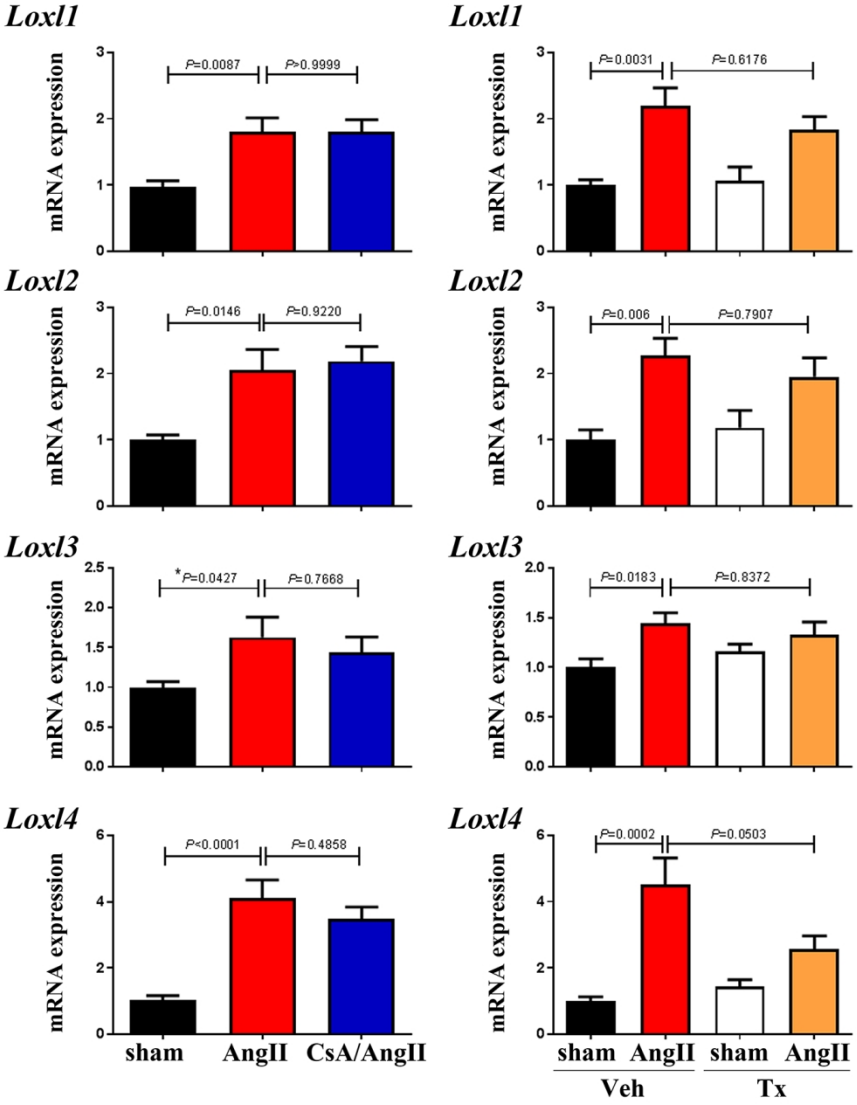
Loxl1
mRNA expression
P=0.0087
P>0.9999
Loxl1
P=0.0031
P=0.6176
Loxl2
P=0.0146
P=0.9220
Loxl2
P=0.006
P=0.7907
Loxl3
*P=0.0427
P=0.7668
Loxl3
P=0.0183
P=0.8372
Loxl4
P<0.0001
P=0.4858
Loxl4
P=0.0002
P=0.0503
sham
AngII
CsA/AngII
sham
AngII
sham
AngII
Veh
Tx

FIGURE 9